PROGRESS REPORT

SUBMITTED UNDER CONTRACT NO. AT-(40-1)-2968

BETWEEN THE

UNITED STATES ATOMIC ENERGY COMMISSION

AND

THE UNIVERSITY OF TENNESSEE

PERIOD

SEPTEMBER 15, 1971 TO AUGUST 15, 1972

Title of Project

RESEARCH CONCERNING IONIC AND FREE RADICAL REACTIONS

IN RADIATION CHEMISTRY

Principal Investigator

T. Ffrancon Williams

Department of Chemistry
University of Tennessee
Knoxville, Tennessee 37916

AEC DOCUMENT

ORO-2968-78

A. Personnel

(1) <u>T. Ffrancon Williams</u>: Professor of Chemistry. Dr. Williams worked 1/4-time during the 1971-72 academic year and full-time during the summer of 1972.

(2) <u>Carolyn M. L. Kerr</u>*: Postdoctoral Research Associate and Instructor. Dr. Kerr worked 1/2-time during the 1971-72 academic year and left the project May 31, 1972.

(3) <u>Jorge A. Wargon</u>: Postdoctoral Research Associate. Dr. Wargon continued with the   : during 1972-72.

(4) <u>Yoon Jin Chung</u>*: Graduate Research Assistant. Dr. Chung received the Ph.D. degree from the University of Tennessee in June, 1972. His doctoral dissertation is entitled "Esr and Optical Studies of Aliphatic Radical Anions and Radical-Anion Pairs in γ-Irradiated Crystalline Solids at Low Temperatures." Dr. Chung left the project June 30, 1972 and is now a postdoctoral research associate at North Carolina State University, Raleigh.

(5) <u>Kenji Takahashi</u>: Graduate Research Assistant. Mr. Takahashi continued with the project during 1972-72.

(6) <u>Kathleen Webster</u>: Graduate Research Assistant. Mrs. Webster continued with the project during 1972-72.

(7) <u>Alan Campion</u>*: Undergraduate Research Assistant on leave from New College, Sarasota, Fla. 33578. Mr. Campion assisted the project in a full-time capacity from September 13, 1971 to March 15, 1972.

Other Personnel (not receiving salary support under this Contract)

(1) Jih Tzong Wang*: Graduate Student. Mr. Wang has been supported by a fellowship grant from the Ministry of National Defense, Republic of China. Dr. Wang received the Ph.D. degree from the University of Tennessee in August, 1972. His doctoral dissertation is entitled "Studies of Hydrogen Atom Abstraction by Methyl Radicals at Low Temperatures in γ-Irradiated Crystalline Organic Compounds." Dr. Wang returns in August, 1972 to Taiwan where he will resume his position in the army of the Republic of China.

(2) Mary Shivar Bonin*: Graduate Student. Mrs. Bonin completed her thesis entitled "Studies of γ-Irradiated n-Butyl Bromide in the Solid State by Optical and Electron Spin Resonance Spectroscopy" and received the M.S. degree from the University of Tennessee in August, 1972.

---

*Denotes persons who have terminated their association with the project.

B. Facilities and Equipment

The office (Room 230) and the main laboratory facilities (Rooms 231-233 and 236) used for this research project are located in Buehler Hall, the new addition to the Department of Chemistry physical plant at the University of Tennessee, Knoxville. Both the ESR spectrometer and the Gammacell-200 cobalt-60 source are now housed in Room 236. These two pieces of equipment together constitute the most essential tools of this research project, and the consolidation of these facilities into one area provides a very convenient experimental setup. The Gammacell was reloaded during 1971 and the unit was away from June 2, 1971 to October 15, 1971. The drive mechanism at the bottom of the Gammacell was damaged during return transit but this damage was rectified and the Gammacell was back in operation from November 12, 1971. The unit has been used continuously since that date without any malfunction.

Items of equipment acquired during the past year included the following:

(1) X-Y recorder from Hewlett-Packard, Model 7001 AM. This recorder is being used in conjunction with the ESR spectrometer for the accurate recording of spectra.

(2) Heater-Sensor Probe from Varian Associates, Part No. 907144. This probe is incorporated in the temperature controller of the variable-temperature accessories for ESR (Varian Associates Model V-4557) and optical work (Optical Cryostat mentioned in last year's report ORO-2968-68).

C. Outline of Progress

During the past year our work has developed along a very broad front. While the program continues to be mainly concerned with intermediate species produced in γ-irradiated organic and inorganic compounds at low temperatures, a completely new thrust has been added through successful ESR studies of radical trapping in the radiolysis of organic liquids. Individual project summaries are given below with appropriate references to published work.

(1) Structural Studies of Aliphatic Radical Anions and Radical-Anion Pairs

A paper[1] summarizing our studies in this area was presented at the Nobel Symposium No. 22 and will be published in the Proceedings of this meeting. Considerable evidence has been obtained that the products of electron attachment can be found in three distinct states as represented by the radical anion, the radical-anion pair, and the separated fragments. For examples and a summary of the interesting interconversion reactions between these states, see p 12 of the attached preprint.[1] Another publication[2] in this area reports on the interesting photodynamic effect which is manifested by reversible line broadening in the esr spectra of the tert-butyl radicals formed in γ-irradiated tert-butyl isothiocyanate. We have also summarized our extensive work on the monomer and dimer radical anions of acetonitrile.[3]

(2) Mechanism of Electron Attachment to Molecules

Additional evidence has been obtained for a strong deuterium isotope effect in the process of electron attachment to acetonitrile

(J. T. Wang, Ph.D. Dissertation, University of Tennessee, August 1972).
Experiments were carried out using mixtures of CH_3CN and CD_3CN in both
crystal 1 and crystal II. Preliminary work has also been done on the
comparison of results from samples which had been γ-irradiated at 77
and 4°K. These findings suggest that this isotope effect is not sensi-
tive to the change of irradiation temperature. If this conclusion is
borne out by further work, it would appear to suggest that electron
capture in this system is not a thermal process and that the isotope
effect does not originate from zero point energy differences. A temper-
ture-independent isotope effect would seem to indicate a mechanism of
electron capture at epithermal energies similar to that proposed by
Demkov (Phys. Letters, 15, 235 (1965)). According to this mechanism,
a transient negative ion experiences a competition between autoioniza-
tion and molecular rearrangement to a stable negative ion, the rate of
the latter process being determined by the nuclear masses involved in
the molecular reorganization. Further experimental work is needed to
evaluate the applicability of this mechanism to the process of electron
capture by acetonitrile.

(3) Hydrogen Atom Abstraction Reactions by Methyl Radicals at
     Low Temperatures

Considerable progress has been made during the past year on this
topic. On the experimental side, comprehensive studies have been
carried out on four different systems. The results obtained in γ-irrad-
iated crystalline methyl isocyanide[4] and in photolyzed methanol glasses[5]

have been written up and accepted for publication. In addition, studies of the hydrogen atom abstraction reaction by methyl radicals in crystal I and crystal II of acetonitrile over a wide range of temperature have been completed using both esr and optical methods (J. T. Wang, Ph.D. Dissertation, University of Tennessee, August 1972; K. Takahashi, M.S. Thesis, in preparation). A theoretical study[6] of the reaction has also been published. Tunneling calculations based on a gaussian potential energy barrier of 10.5 kcal mol^{-1} provide a very satisfactory description of the abstraction reactions in CH_3NC and CH_3CN (crystal I and crystal II) between ca. 70 and 120°K. The tunneling effect is very sensitive to the barrier width and slightly different barrier widths are found for these reactions. In particular it should be noted that the difference between the results for the reaction in crystal I and crystal II of acetonitrile can be wholly accounted for by a change in the width parameter. This is a most reasonable result considering that the only difference to be expected is that concerning the geometrical disposition of the reactants in the two crystalline states. Full details of the experimental and theoretical results are presented in Wang's dissertation.

(4) Electron Spin Resonance Studies of γ-Irradiated Phosphorus
      and Sulfur Compounds

The radical anions of phosphorus oxychloride[7] and sulfuryl chloride[8] have been identified. The complete account of our work on $SO_2Cl_2^{-}$ has just appeared in press,[8] and describes results obtained in the cryst-

alline compound and in several organic glasses. The structure of $SO_2Cl_2^-$ can best be represented as a radical anion complex of sulfur dioxide and chlorine, in which the unpaired electron is associated with the lowest unoccupied orbitals of both molecules, so that there is appreciable spin density on all five atoms. It is of interest to note that our recent work has revealed two other clear examples of weakly bonded radical anion complexes, viz., the dimer radical anion of acetonitrile[3] and the methyl radical-bromide ion pair (E. D. Sprague and F. Williams, J. Chem. Phys., 54, 5425 (1971)).

Our studies of γ-irradiated phosphorus compounds have been extended. Evidence has been obtained for alkyl radical formation by dissociative electron capture in alkyl phosphate esters.[9] Also a variety of radicals formed at 77°K in γ-irradiated compounds containing phosphorus and chlorine have been identified by their esr spectra. Competitive scavenging experiments[9] using samples doped with methyl bromide have been used to indicate which of the radicals are formed by electron capture. Confirmatory studies have been made on solutions in organic glasses which on γ irradiation yield the products of electron capture. From this work, it has been found that compounds of formula $Cl_2P(O)X$, where X = Cl, OC_2H_5, or C_6H_5, undergo non-dissociative electron capture to form radical anions. In contrast to this, $(C_2H_5O)_2P(O)Cl$ yields a mixture of $(C_2H_5O)_2\overset{\bullet}{P}O$ and $C_2H_5O\overset{\bullet}{P}(O)Cl$ radicals, the latter being formed by dissociative electron capture. Similar studies have also been carried out on phosphite and pyrophosphite esters and definitive esr evidence has been obtained for

a wide variety of phosphorus-centered radicals. The results of this work are being prepared for publication.

(5) Electron Spin Resonance Studies of Radical Trapping in the
Radiolysis of Organic Liquids

We have recently applied the technique of "spin trapping" to the radiolysis of organic liquids. The first report[10] deals with evidence for the primary formation of the methoxy radical in methanol. The radicals were trapped using 2-methyl-2-nitrosopropane and nitroxide radicals corresponding to the addition of $CH_3O\cdot$ and $\cdot CH_2OH$ were clearly identified by esr spectroscopy from the ^{14}N and ^1H hfs. The dependence of the results on the concentration of scavenger indicates that $CH_3O\cdot$ is the most abundant primary radical produced in the radiolysis and that $\cdot CH_2OH$ is formed by a secondary reaction involving H atom abstraction by $CH_3O\cdot$ from CH_3OH. In the presence of methyl bromide, additional esr lines belonging to the spectrum of the methyl tert-butyl nitroxide radical were identified showing that methyl radical formation had occurred through electron scavenging by CH_3Br. These results clearly demonstrate the usefulness of the spin trapping method in radiation chemistry and further work is now in progress on a variety of organic compounds including alcohols, ethers, and thiols.

(6) Pulse Radiolysis Studies

A pulse radiolysis study of succinonitrile in the rotator phase[11] is in the course of publication. This work was carried out in collaboration with Dr. J. A. Ghormley using the pulse radiolysis facilities at the Oak Ridge National Laboratory.

(7) <u>Miscellaneous</u>

(a) <u>On the Discovery of $H_3O\cdot$</u>

Contrary to the previous report (T. W. Martin and L. L. Swift, <u>J.</u> <u>Amer</u>. <u>Chem</u>. <u>Soc</u>., <u>93</u>, 2788 (1971)), no evidence was obtained for $H_3O\cdot$ and $D_3O\cdot$ radicals in UV-irradiated perchloric acids containing ceric ion.[12] It is suggested that the previously observed spectrum which was assigned to $H_3O\cdot$ is that of the $CH_3\cdot$ radical, presumably formed by the photo-oxidation of impurities.

(b) <u>Structure of the Hydrated Electron</u>

We have recently employed the INDO method to investigate the structure of the hydrated electron using a comparison of the experimental and theoretical spin densities on the hydrogen nuclei as a criterion of structural validity.[13] This approach stems directly from our recent work on radical anion complexes.[3,8]

(c) <u>Radiation-Induced Polymerization</u>

The U.S. Patent Office granted a patent[14] to the Atomic Energy Commission based on the extensive work performed in the course of this contract on radiation-induced ionic polymerization.

D. <u>Publications</u>

The following reprints and preprints for the period under review are appended to this report, and these documents are numbered so as to correspond with the references made in the preceding outline of progress.

(1) [ORO-2968-76] "ESR Studies of Aliphatic Radical Anions and Radical-Anion Pairs in γ-Irradiated Crystalline Solids" by M. A. Bonin, Y. J. Chung, E. D. Sprague, K. Takeda, J. T. Wang, and F. Williams, Proceedings of Nobel Symposium, No. 22, in press (1972).

(2) [ORO-2968-73] "Reversible Line Broadening in the Electron Spin Resonance Spectra of tert-Butyl Radicals in γ-Irradiated Crystalline tert-Butyl Isothiocyanate by Y. J. Chung and F. Williams, J. Phys. Chem., 76, 1792 (1972).

(3) [ORO-2968-61] "The Dimer Radical Anion of Acetonitrile" by E. D. Sprague, K. Takeda, and F. Williams, Chem. Phys. Lett., 10, 299 (1971).

(4) [ORO-2968-65] "Hydrogen Atom Abstraction by Methyl Radicals in γ-Irradiated Crystalline Methyl Isocyanide at 77-125°K" by J. T. Wang and F. Williams, J. Amer. Chem. Soc., 94, 2930 (1972).

(5) [ORO-2968-74] "Hydrogen Atom Abstraction by Methyl Radicals in Methanol Glasses at 67-77°K" by A. Campion and F. Williams, J. Amer. Chem. Soc., 94, in press (1972).

(6) [ORO-2968-64] "Quantum Mechanical Tunneling in Hydrogen Atom Abstraction from Solid Acetonitrile at 77-87°K" by R. J. Le Roy, E. D. Sprague, and F. Williams, J. Phys. Chem., 76, 546 (1972).

(7) [ORO-2968-63] "Electron Spin Resonance Spectrum and Structure of the Radical Anion of Phosphorus Oxychloride" by C. M. L. Kerr and F. Williams, J. Phys. Chem., 75, 3023 (1971).

(8) [ORO-2968-70] "Electron Spin Resonance, Optical, and Theoretical Studies of the Radical Anion of Sulfuryl Chloride" by C. M. L. Kerr and F. Williams, J. Amer. Chem. Soc., 94, 5212 (1972).

(9)) [ORO-2968-72] "Electron Spin Resonance Evidence for Dissociative Electron Capture in γ-Irradiated Phosphate Esters" by C. M. L. Kerr, K. Webster, and F. Williams, J. Phys. Chem., 76, in press (Sept. 28, 1972).

(10) [ORO-2968-77] "Electron Spin Resonance Studies of Radical Trapping in the Radiolysis of Organic Liquids. I. Evidence for the Primary Formation of the Methoxy Radical in Methanol" by J. A. Wargon and F. Williams, submitted for publication.

(11) [ORO-2968-71] "Pulse Radiolysis Study of Succinontrile in the Rotator Phase" by A. Campion, J. A. Ghormley, and F. Williams, J. Amer. Chem. Soc., 94, 6301-4 in press (Sept. 6, 1972).

(12) [ORO-2968-69] "On the Reported Discovery of the Hydronium Radical in ESR Studies of UV-Irradiated Perchloric Acid Glasses Containing Ceric Ion" by J. A. Wargon and F. Williams, Chem. Phys. Lett., 13, 579 (1972).

(13) [ORO-2968-75] "An Investigation of the Structure of the Hydrated Electron based on Unpaired Electron Densities Calculated by the INDO Method" by C. M. L. Kerr and F. Williams, J. Phys. Chem., 76, in press (December, 1972).

(14) "Radiation-Induced Ionic Polymerization Controlled by the Presence of Lewis Acids or Lewis Bases" by T. F. Williams, U.S. Patent 3,616,369, October 26, 1971.

In addition to the above list of papers, the following review chapters have been published. The manuscripts were included in last year's report [ORO-2968-68].

(15) [ORO-2968-66] "Early Processes in Radiation Chemistry and the Reactions of Intermediates" by F. Williams, in "The Radiation Chemistry of Macromolecules," Ed. M. Dole, Academic Press, New York, 1972, Chapter 2, pp 7-23.

(16) [ORO-2968-67] "ESR and Optical Studies of Trapped Electrons in Glasses and Polymers" by R. M. Keyser, K. Tsuji, and F. Williams, in "The Radiation Chemistry of Macromolecules," Ed. M. Dole, Academic Press, New York, 1972, Chapter 9, pp 145-191.

E. Dissertations and Theses

(1) Ph.D. Dissertation, "ESR and Optical Studies of Aliphatic Radical Anions and Radical-Anion Pairs in γ-Irradiated Crystalline Solids at Low Temperatures" by Yoon Jin Chung (University of Tennessee, June 1972).

(2) Ph.D. Dissertation, "Studies of Hydrogen Atom Abstraction by Methyl Radicals at Low Temperatures in γ-Irradiated Crystalline Organic Compounds" by Jih Tzong Wang (University of Tennessee, August 1972).

(3) M.S. Thesis, "Studies of γ-Irradiated n-Butyl Bromide in the Solid State by Electron Spin Resonance and Optical Spectroscopy" by Mary Shivar Bonin (University of Tennessee, August 1972).

F. Participation in Meetings

(1) Paper D2 (presented by C. M. L. Kerr) contributed at the 3rd Southeastern Magnetic Resonance Conference, Oak Ridge, Tennessee, October 20-22, 1971. The paper was entitled "The Radical Anion of Sulfuryl Chloride" by C. M. L. Kerr and F. Williams.

(2) Attended Conference on "Elementary Processes in Radiation Chemistry" at the University of Notre Dame, Indiana, April 4-7, 1972. Chairman of Session VIII on "Ionic Processes in Solids."

(3) Invited speaker at Nobel Symposium No. 22 on "ESR Applications to Polymer Research" at Södergarn, Lidingö, Stockholm, Sweden, June 20-22, 1972. The paper (No. 10) was entitled "ESR Studies of Aliphatic Radical Anions and Radical-Anion Pairs in γ-Irradiated Crystalline Solids."

Electron Spin Resonance Evidence for·Dissociative Electron Capture in γ-Irradiated Phosphate Esters[1]

by Carolyn M. L. Kerr, Kathleen Webster, and Ffrancon Williams[*]

Department of Chemistry, University of Tennessee, Knoxville, Tennessee 37916

(Received   )

Alkyl radicals are formed during γ-irradiation of alkyl phosphates at 77°K.
Inclusion of an electron scavenger virtually eliminates this reaction and
a comparable yield of radicals derived from the scavenger is obtained. This
proves that alkyl radicals are formed only by dissociative electron capture
in the pure esters. Possible biological implications are discussed.

Introduction

The mechanism of interaction of ionizing radiation with phosphate esters is of interest as these compounds are closely related to many important constituents of biological materials. The effect of γ-irradiation on alkyl phosphates has been investigated by product analysis,[2] and more recently by esr examination of the radical intermediates at low temperatures.[3,4] Although various reaction steps have been postulated on the basis of the information obtained, definitive proof of these is lacking. Here we present the results of an esr study which demonstrates conclusively that the alkyl radicals observed in γ-irradiated alkyl phosphates are formed by dissociative electron capture. This finding confirms a previous suggestion along these lines.[4]

Experimental Section

Trimethyl phosphate, triethyl phosphate, dimethyl methyl phosphonate, and dimethyl acid pyrophosphate were supplied by Aldrich Chemical Co. and used without purification. Samples of each compound were prepared both with and without a quantity of a known electron scavenger,[5] ethyl bromide being used as the scavenger for the methyl esters and methyl bromide for the ethyl ester. The alkyl halide concentration was nominally 1 mole % or greater. It was found necessary to use low ethyl bromide concentrations (1-2 mole %) to avoid formation of the $\cdot C_2H_4Br$ radical since its spectrum tended to obscure that of the ethyl radical. All samples formed glasses when quenched to 77°K. The doped and undoped samples of each compound were irradiated

at this temperature to the same total dose (0.1 to 0.2 Mrad), and their esr

spectra recorded immediately using identical spectrometer conditions. The

esr spectrometer and accessories have been described elsewhere.[6]

Results and Discussion

In all the methyl esters that were examined, the quartet esr spectrum

of the methyl radical ($A_{iso}^{CH_3}$ = 23 G) was superimposed on a broad triplet

which can be assigned to the O=P-O-$CH_2\cdot$ radical.[7] On the other hand, the

somewhat anisotropic twelve-line spectrum obtained in the sample doped

with ethyl bromide appeared to be mainly due to the ethyl radical ($A_{iso}^{CH_3}$ =

27 G, A^{CH_2} = 21 G), indicating that a large fraction of the electrons had

been captured by the ethyl bromide. Representative spectra obtained for

trimethyl phosphate are shown in Figures 1A and 1B, with stick diagrams

indicating the spectral analyses.[8] Although the spectra of the two radicals

are quite different, the positions of the four lines in the methyl radical

spectrum lie close to those of lines 3, 5, 8 and 10 of the ethyl radical

spectrum, thus rendering a relatively small amount of methyl radical difficu[l]

to detect in the presence of ethyl. However, the methyl radicals disappeared

rapidly at 77°K so that any contribution to the spectrum in the doped

sample could be determined by recording the spectrum again after the

decay was observed to be complete in the spectrum of the pure sample

(Figure 1C). The corresponding spectrum of the doped sample is shown

in Figure 1D. Comparison of Figures 1B and 1D shows that the intensities

of lines 3 and 10 relative to the adjacent outer lines (which are due

only to the ethyl radical) are diminished in Figure 1D. The difference, however, represents only a small contribution to the initial spectrum by methyl radicals, and scavenging is probably better than 90% complete. Results similar to the above were obtained for the phosphonate and acid pyrophosphate. In the case of the triethyl phosphate, ethyl radicals were observed in the pure material and methyl in the doped sample. As the ethyl radical signal was almost unchanged after six days whereas the methyl had decayed out leaving no trace of ethyl, scavenging by methyl bromide was judged to be complete.

Since complete scavenging was observed for triethyl phosphate containing ~8 mole % of methyl bromide, it is reasonable to assume that the incomplete scavenging occurring in the methyl esters was due to the much lower (1-2 mole %) scavenger concentration used in this case. The fact that the parent alkyl radical is largely but not completely replaced by radicals derived from the scavenger when the latter is present in low concentration is evidence for competition between the highly efficient ethyl bromide[5a] and the methyl esters for the electrons. The observation of comparable yields of parent alkyl and scavenger alkyl radicals in the doped and undoped samples further indicates that the parent alkyl radicals originate from dissociative electron capture by the phosphate esters. The reaction can be written as follows, where $R = CH_3$ or C_2H_5:

$$O=\overset{\displaystyle |}{\underset{\displaystyle |}{P}}-O-R + e^- \longrightarrow O=\overset{\displaystyle |}{\underset{\displaystyle |}{P}}-O^- + R\cdot$$
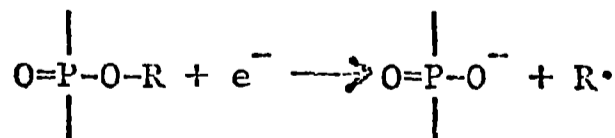
Although it is clear to us that the results reported here provide definitive evidence for the formation of parent alkyl radicals from the phosphate esters by dissociative electron capture, this interpretation has been questioned by one of the Reviewers of this paper. Therefore some elaboration seems to be necessary. If we assume that the parent alkyl radicals are not formed by dissociative electron capture, then the presence of an electron scavenger should not affect their initial formation and these radicals must be removed by a rapid (i.e., unobservable) secondary reaction with the scavenger. This would require that methyl radicals (which decay only slowly in the absence of scavenger[7]) react with ethyl bromide and that ethyl radicals react with methyl bromide. The only reasonable course of these reactions would involve radical displacement, and since one is the reverse of the other, it is difficult to understand why both should proceed efficiently. Therefore, this alternative explanation to dissociative electron capture may be dismissed.

The present findings may have some bearing on the mechanism of radiation damage in biological molecules containing phosphate ester linkages. For example, dissociative electron capture processes similar to those observed here could bring about main chain scission in polynucleotides. A significant feature of this process is that the products are very unlikely to to recombine. This is in contrast to the case of homolytic fission where two free radicals are formed adjacent to one another and a repair mechanism is feasible. Another aspect of this study which deserves comment is the possibility that the incorporation of suitable electron scavengers might be useful in protecting biological material from inactivation by radiation.

References

(1) This work was supported by the U.S. Atomic Energy Commission under Contract No. AT-(40-1)-2968, and this is AEC Document No. ORO-2968-72.

(2) R. W. Wilkinson and F. Williams, *J. Chem. Soc.*, 4098 (1961).

(3) S. Sugimoto, K. Kuwata, S. Ohnishi, and I. Nitta, *Rep. Jap. Assoc. Rad. Res. Polymers*, 7, 199 (1965-1966).

(4) A. Begum, S. Subramanian, and M. C. R. Symons, *J. Chem. Soc.*, A, 1334 (1970).

(5) (a) J. M. Warman, K.-D. Asmus, and R. H. Schuler, "Radiation Chemistry-II," Advances in Chemistry Series, No. 88, American Chemical Society, Washington, D.C., 1968, pp. 25-57; (b) E. D. Sprague and F. Williams, *J. Chem. Phys.*, 54, 5425 (1971).

(6) J. Lin, K. Tsuji, and F. Williams, *J. Amer. Chem. Soc.*, 90, 2766 (1968).

(7) Since the yield of the $O=\overset{|}{\underset{|}{P}}-O-CH_2\cdot$ radical from trimethyl phosphate is considerably smaller in the sample doped with ethyl bromide than in the undoped sample (Figure 1), it is very probable that this radical originates largely from the decay of methyl radicals by hydrogen atom abstraction from the trimethyl phosphate. For other examples of hydrogen atom abstraction by methyl radicals at 77°K see (a) E. D. Sprague and F. Williams, *J. Amer. Chem. Soc.*, 93, 787 (1971); (b) R. J. Le Roy, E. D. Sprague, and F. Williams, *J. Phys. Chem.*, 76, 546 (1972); (c) J.-T. Wang and F. Williams, *J. Amer. Chem. Soc.*, 94, 0000 (1972); (d) A. Campion and F. Williams, submitted for publication.

(8) In the powder spectrum of the ethyl radical (Figure 1D), the signal heights of the sharp lines (2, 5, 8, and 11) are enhanced relative to the heights of the other lines as compared to the intensity ratios indicated in the stick diagram. This is due to a line-width difference which arises from anisotropic hyperfine broadening. For a detailed explanation, see E. L. Cochran, F. J. Adrian, and V. A. Bower, *J. Chem. Phys.*, 34, 116ī (1961).

FIGURE CAPTION

Figure 1.   Esr spectra of γ-irradiated trimethyl phosphate with and without ethyl bromide.   The radiation dose was 0.2 Mrad.   All spectra were recorded at 77°K under the same spectrometer conditions.   The spectra refer to samples as follows:

A.   Pure trimethyl phosphate immediately after γ-irradiation.

B.   Trimethyl phosphate containing 1-2 mole % ethyl bromide immediately after γ-irradiation.

C.   Same sample as 1A six days after irradiation.

D.   Same sample as 1B six days after irradiation.
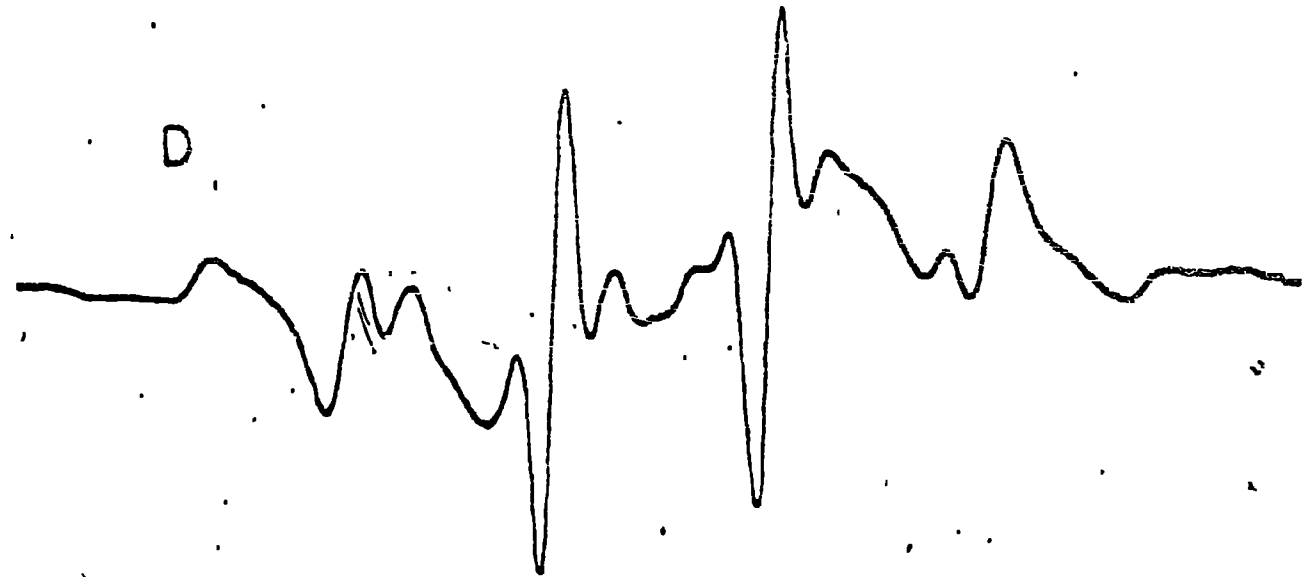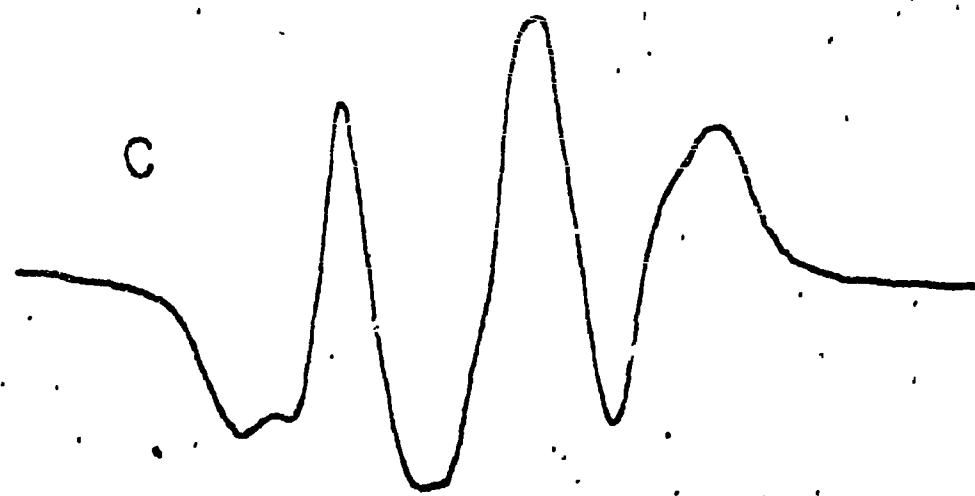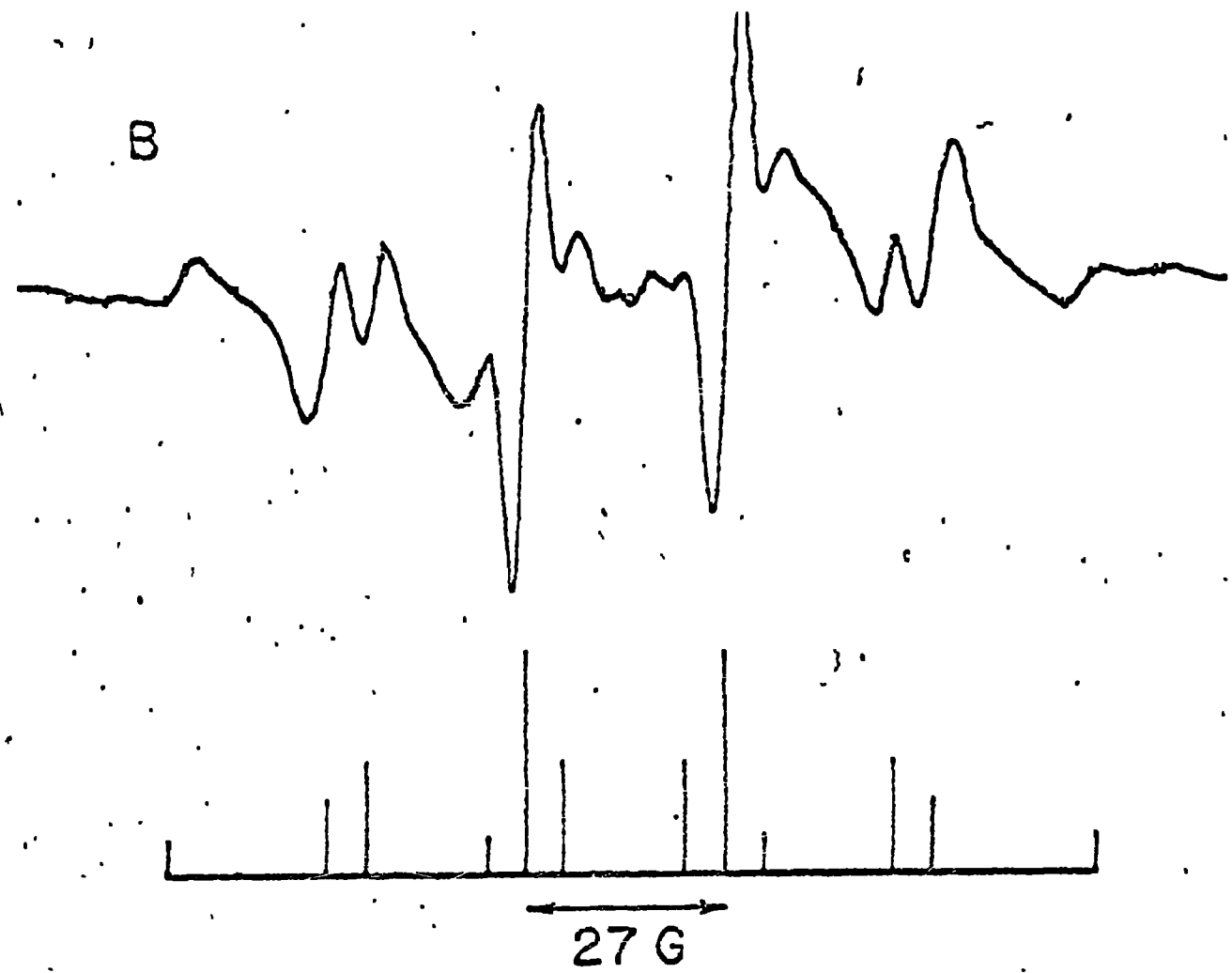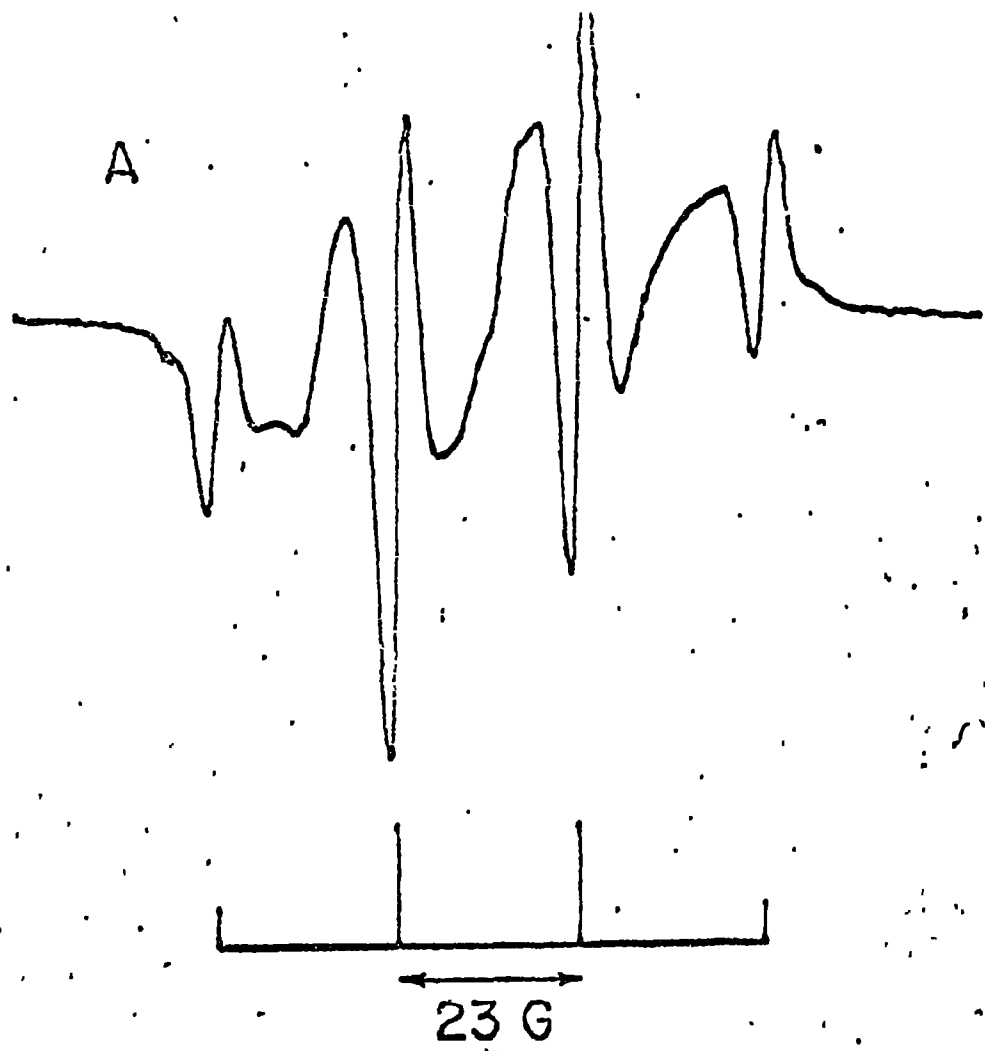
Figure 1   Kerr, Webster, and Williams
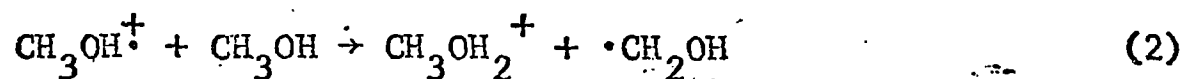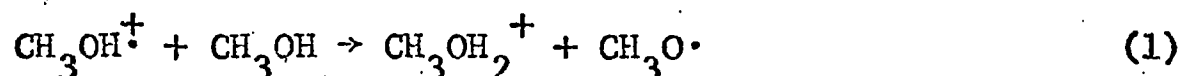
Electron Spin Resonance Studies of Radical Trapping in the Radiolysis of Organic Liquids. I. Evidence for the Primary Formation of the Methoxy Radical in Methanol[1]

Sir:

Although the technique of "spin trapping"[2] (radical trapping followed by esr identification of a more stable adduct radical) has been employed successfully in recent years for the study of free radical intermediates in chemical reactions,[2-4] its application to radiation chemistry seems to have been limited heretofore to the irradiation of solids[5] and aqueous solutions.[6] We now wish to report on the utilization of this technique to resolve the persistent problem of primary radical formation in the radiolysis of deaerated liquid methanol.[7,8]

It has been widely suggested[7] that the facile ion-molecule reactions (1) and (2) contribute to radical formation in the radiolysis of methanol.

$$CH_3OH^{+} + CH_3OH \rightarrow CH_3OH_2^{+} + CH_3O\cdot \qquad (1)$$

$$CH_3OH^{+} + CH_3OH \rightarrow CH_3OH_2^{+} + \cdot CH_2OH \qquad (2)$$

Mass spectroscopic studies[9,10] show that these reactions occur with about equal probability in the vapor, but this result may not apply to the liquid phase where strong hydrogen bonding is present. Accordingly, information is desirable about the initial distribution of radicals in the liquid. Previous studies[7,8] have provided abundant evidence for the participation

of the hydroxymethyl radical in the radiation chemistry of liquid and solid methanol, but it has been recognized[7] that this radical could also be produced by other processes including the secondary reaction (3)

$$CH_3O\cdot + CH_3OH \rightarrow CH_3OH + \cdot CH_2OH \qquad (3)$$
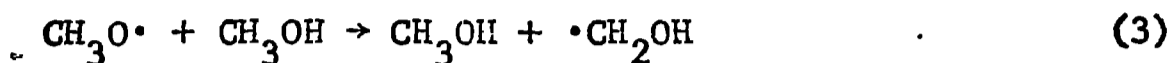
from a methoxy radical precursor. However, definitive proof of methoxy radical formation has been lacking although its intermediacy was inferred from the analysis of reaction products derived from the radiolysis of benzene-methanol mixtures,[11] and more recently from the pulse radiolysis detection of an oxidizing species.[12]

In this work we have used 2-methyl-2-nitrosopropane $((CH_3)_3C-N=O$, I) as a radical trap[3,4] to produce nitroxide radicals according to reaction (4).

$$\cdot R\cdot + (CH_3)_3C-N=O \rightarrow \begin{array}{c} R \\ (CH_3)_3C \end{array} \!\!\!\! N-O\cdot \qquad (4)$$
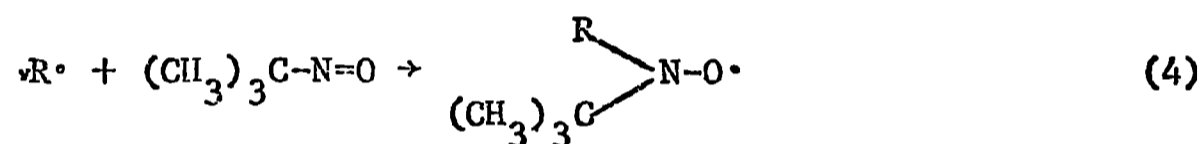
The esr hyperfine structure of these nitroxides is generally characteristic of the trapped radical and identification is straightforward, as described below. Figure 1 shows esr spectra recorded after γ irradiation of solutions containing different concentrations of I in methanol at $-78°$. The upper spectrum obtained at the higher scavenger concentration (10^{-1} $\underline{M}$ based on complete dissociation of the dimer[13]) consists almost exclusively of a ^{14}N triplet of 1:3:3:1 quartets indicating hfs from three equivalent hydrogens in the trapped radical. Assignment of these lines to the methoxy tert-butyl nitroxide ($\begin{array}{c} CH_3O \\ (CH_3)_3C \end{array} \!\!\!\! N-O\cdot$, II) follows from the magnitude of the nitrogen splitting which is characteristic of alkoxy radical addition

to I,[4b] and from the close correspondence of the hyperfine constants a^N = 29.7 G and a^H = 1.6 G to the values of 29.4 and 1.4 G reported[3b] for the similar nitroxide radical produced by methoxy radical addition to 2-methyl-2-nitrosobutan-3-one. The lower spectrum in Figure 1 corresponding to the smaller scavenger concentration of 10^{-2} $\underline{M}$ shows that the lines from II are now accompanied by another prominent set of components (^{14}N triplet of 1:2:1 triplets) which are readily identified as belonging to the hydroxymethyl tert-butyl nitroxide (

$$\begin{array}{c} HOH_2C \\ (CH_3)_3C \end{array} \Big\rangle N\!-\!O\cdot, \ III),$$ the

values of the hyperfine constants, a^N = 14.5 G and a^H = 4.1 G, being in good agreement with those previously reported for this radical.[4b,14] Comparison of the two spectra shows that lines from III are barely discernible in the upper spectrum.

Parallel results were obtained from experiments with CH_3OD and CD_3OD at -78°. As expected, the esr spectra of the nitroxides produced from CH_3OD were virtually identical to those described from CH_3OH. In the case of CD_3OD the spectra were again easily analyzed since the simple triplets from the anticipated nitroxides corresponding to II and III can be readily distinguished by virtue of the large difference in the ^{14}N splittings.

The esr spectra were always recorded at -80° immediately after γ irradiation of the samples at -78° for 10 min (dose = 0.07 Mrad). The signal due to II decreased very slowly at this temperature whereas the signal from III remained constant, ruling out the possibility of interconversion between these two isomeric nitroxide radicals. At higher

temperatures the decay of II was especially marked, and when the entire

experiments were carried out at 25° only the spectrum of III was observed

irrespective of the scavenger concentration. The thermal instability

of alkoxy nitroxides has been noted previously.[15] Consequently, no

conclusions can be drawn about the radiolysis mechanism from radical trap-

ing experiments carried out with I above -80°.

The concentration dependence of the esr results at -80° strongly

indicates that the hydroxymethyl radical arises almost entirely from the

secondary reaction (3) in competition with the scavenging of methoxy

radicals by reaction (4). A similar competition was previously suggested[12]

to explain the high concentration (10^{-1} $\underline{M}$) of iodide ion necessary for

complete scavenging of the oxidizing species, presumed to be the methoxy

radical, in methanol radiolysis.

Evidently the methoxy radical is the most abundant primary radical

produced in the radiolysis of liquid methanol. In order to probe the

mechanism of its formation, further experiments were carried out using

10^{-1} $\underline{M}$ solutions of I containing a high concentration (1-5 mol percent) of

methyl bromide, an excellent electron scavenger.[16] The esr results showed

that the formation of II was unaffected by the presence of the methyl

bromide, while additional lines belonging to the spectrum of methyl tert-

butyl nitroxide[3b,4b] (
$$\begin{array}{c} CH_3 \\ \diagdown \\ (CH_3)_3C \diagup \end{array} N{-}O\cdot,\ IV)$$
were easily identified.

The appearance of IV in this system is diagnostic of methyl radical for-

mation through electron scavenging by the methyl bromide,[16] and therefore

these results show that the methoxy radical does not originate from

electron attachment or ion recombination processes. It follows that the present work is entirely consistent with the formation of the methoxy radical by reaction -(1) and that relative to the gas phase results, reaction (2) is much less important than reaction (1). Consequently, it would appear that the hydrogen bonding in the liquid phase facilitates the selective transfer of the hydroxyl hydrogen in the primary ion-molecule reaction.

These results illustrate the potential usefulness of the spin trapping technique as applied to the radiolysis of organic liquids where more than one type of radical is commonly produced.[17] Mention should also be made of the fact that no nitroxide radicals originated from a radiation-induced decomposition of I, in contrast to the photolysis at certain wavelengths.[2c] Finally, the high sensitivity of the technique means that results can be obtained at relatively low radiation doses (<0.1 Mrad), thereby avoiding the risk of complications resulting from the buildup of radiolysis products.

Jorge A. Wargon,[18] Ffrancon Williams[*19]
Department of Chemistry, University of
Tennessee, Knoxville, Tennessee 37916

Received

REFERENCES

(1)   This research was supported by the U.S. Atomic Energy Commission under Contract No. AT-(40-1)-2968, and this is AEC Document No. ORO-2968-77.

(2)   (a) E. G. Janzen and B. J. Blackburn, J. Amer. Chem. Soc., 90, 5909 (1968); (b) E. G. Janzen and B. J. Blackburn, ibid., 91, 4481 (1969); (c) E. G. Janzen, Accounts Chem. Res., 4, 31 (1971).

(3)   (a) C. Lagercrantz and K. Torssell, Acta Chem. Scand., 22, 1935 (1968); (b) S. Forshult, C. Lagercrantz, and K. Torssell, ibid., 23, 522 (1969); (c) C. Lagercrantz, J. Phys. Chem., 75, 3466 (1971).

(4)   (a) G. R. Chalfont, M. J. Perkins, and A. Horsfield, J. Amer. Chem. Soc, 90, 7141 (1968); (b) M. J. Perkins, P. Ward, and A. Horsfield, J. Chem. Soc. (B), 395 (1970); (c) M. J. Perkins, Chem. Soc. Spec. Publ., No. 24, Chapter 5, 97 (1970).

(5)   C. Lagercrantz and S. Forshult, Nature, 218, 1247 (1968).

(6)   (a) K. Eiben and R. W. Fessenden, J. Phys. Chem., 72, 3387 (1968); (b) D. Behar and R. W. Fessenden, ibid., 76, 1710 (1972).

(7)   F. S. Dainton, G. A. Salmon, and P. Wardman, Proc. Royal Soc. (London) A, 313, 1 (1969).

(8)   G. R. Freeman in "Actions Chimiques et Biologiques des Radiations," M. Haissinsky, Ed., Volume 14, Masson et Cie., Paris, 1970, Chapter II, p. 73.

(9)   J. C. J. Thynne, J. K. Amenu-Kpodo, and A. G. Harrison, Can. J. Chem., 44, 1655 (1966).

(10) D. J. Hyatt, E. A. Dodman, and M. J. Henchman, Advan. Chem. Ser., No. 58, 131 (1966).

(11) A. Ekstrom and J. L. Garnett, J. Phys. Chem., 70, 324 (1966).

(12) F. S. Dainton, I. Janovsky, and G. A. Salmon, Chem. Commun., 335 (1969).

(13) (a) The compound exists as a trans dimer in the solid state; see I. T. Millar and H. D. Springall, "The Organic Chemistry of Nitrogen by the late N. V. Sidgwick," Clarendon Press, Oxford, 1966, Chapter 10, p 343; (b) the monomer-dimer equilibrium in methanol is being studied by nmr spectroscopy. Contrary to a previous statement[4b] we find that photo-activation is not necessary to bring about the dissociation of the dimer at -80°.

(14) I. H. Leaver and G. C. Ramsay, _Tetrahedron_, 25, 5669 (1969).

(15) A. Mackor, Th. A. J. Wajer, Th. J. de Boer, and J. D. W. van Voorst, _Tetrahedron Lett._, 385 (1967).

(16) (a) J. M. Warman, K.-D. Asmus, and R. H. Schuler, _Advan. Chem. Ser._, No. 88, 25 (1968); (b) E. D. Sprague and F. Williams, _J. Chem. Phys._, 54, 5425 (1971).

(17) R. A. Holroyd in "Fundamental Processes in Radiation Chemistry," P. Ausloos, Ed., Wiley, New York, N.Y., 1968, Chapter 7, p 413.

(18) Fellow of the Consejo Nacional de Investigaciones Cientificas y Tecnicas, Republic of Argentina.

(19) John Simon Guggenheim Memorial Foundation Fellow, 1972-73.

Figure Caption

Figure 1. Esr first-derivative spectra of methanol solutions of 2-methyl-2-nitrosopropane recorded at −80° after γ irradiation for 10 min (dose, 0.07 Mrad) at −78°. The upper and lower spectra refer to concentrations of 10^{-1} and 10^{-2} $\underline{M}$, respectively. In addition to the components indicated by the stick diagram (see text), the upper spectrum shows a triplet ($\underline{a}^N = \underline{ca}$. 16.2 G) of very weak lines; these lines were also observed before γ irradiation and belong to di tert-butyl nitroxide formed during preparation of the sample.
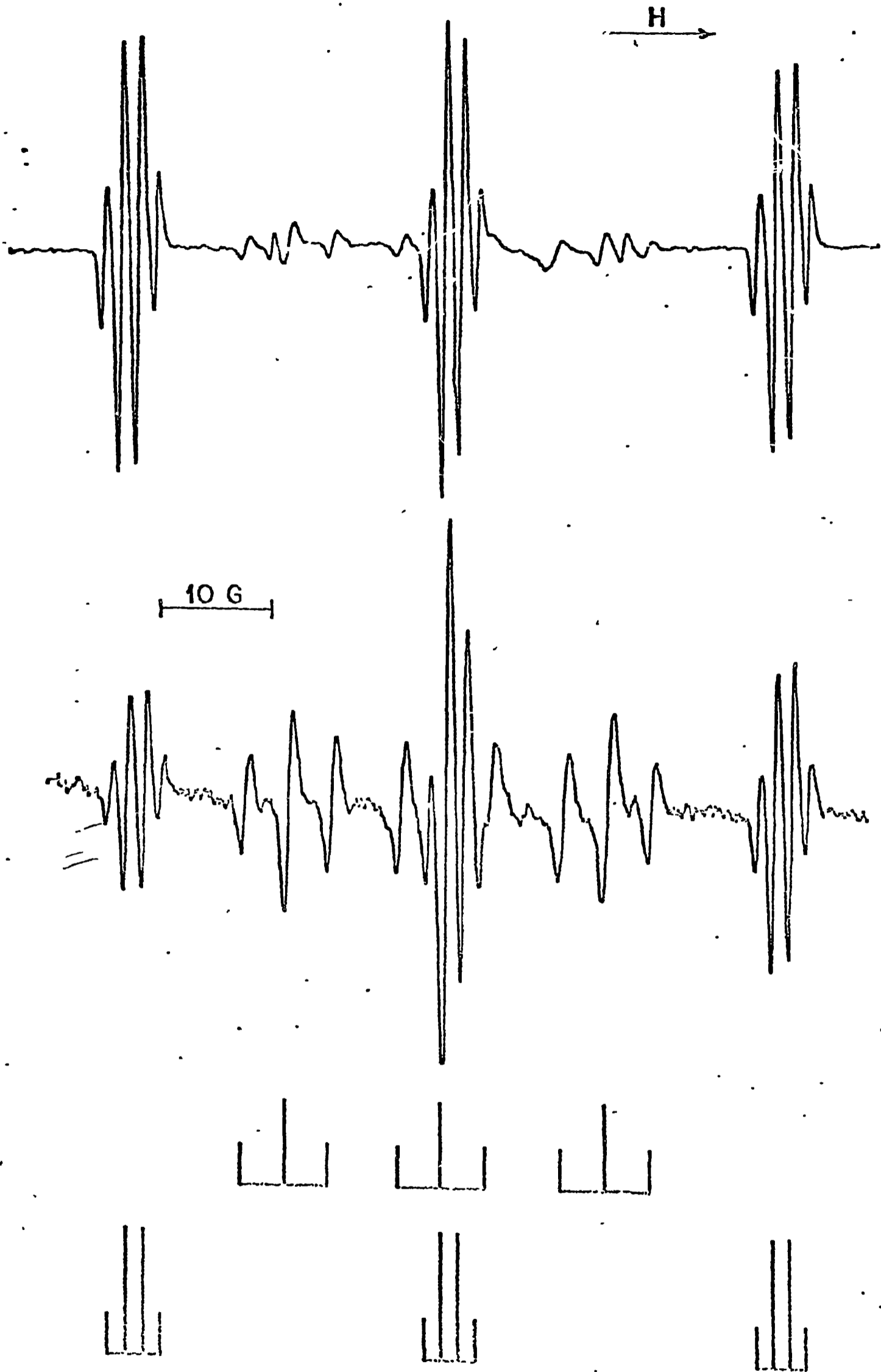
Figure 1. Wargon and Williams

A Pulse Radiolysis Study of Succinonitrile in the Rotator Phase[1,2]

Alan Campion,[3a] John A. Ghormley,[3b] and Ffrancon Williams[3c]*

Contribution from the Chemistry Division, Oak Ridge National Laboratory, Oak Ridge, Tennessee 37830, and the Department of Chemistry, The University of Tennessee, Knoxville, Tennessee 37916. Received

Abstract: A transient absorption spectrum ($t_{1/2}$ = 0.23 μsec) has been detected in the pulse radiolysis of succinonitrile, a plastic crystal at room temperature. This absorption is not produced in the presence of 1 mole % tetracyanoethylene (TCNE) and the spectrum of TCNE⁻ is observed instead. The value of λ_{max} (450 nm) for the transient corresponds to the absorption maxima observed in the low temperature spectra of monomer radical anions from acetonitrile and adiponitrile. On the basis of these results, the transient spectrum is assigned to a monomer radical anion of succinonitrile although the possibility of a dimer species similar to that observed at low temperature cannot be excluded. The first order decay of the radical anion is attributed to the unimolecular dissociation to $\cdot CH_2CH_2CN$ and CN^- . In addition to the radical anion, a long-lived species is produced which absorbs most strongly in the ultraviolet.

1

In the pulse radiolysis of organic liquids, studies of transient ions by optical absorption spectroscopy have been largely restricted to solvated electrons and to ions produced by reactions with suitable charge scavengers.[4] The detection of these ions is facilitated by a $\underline{G}$ ε_{max} product which frequently exceeds 1×10^4, where $\underline{G}$ is the 100 eV yield of species with lifetimes exceeding the resolution time of the equipment and ε_{max} is the extinction coefficient in $\underline{M}^{-1}$ cm^{-1} at the absorption maximum (λ_{max}). Two pulse radiolysis studies of acetonitrile solutions containing aromatic hydrocarbons such as biphenyl[5] and anthracene[6] have been reported in which transient absorption spectra were readily observed and identified as belonging to the radical anion and triplet state of the solute. For pure acetonitrile, however, there is only a brief report[5] of a short-lived transient $(\underline{t}_{1/2} < 5$ µsec) with a very weak absorption at 660 nm which was tentatively attributed to a solvated electron. Even this observation is in doubt because in a later study of the pulse radiolysis of oxygen-free acetonitrile,[6] no absorption could be detected between 280 and 800 nm despite high sensitivity and a resolution time of 100 nsec.

By contrast, esr and optical studies of γ-irradiated acetonitrile in the solid state at low temperature have definitely shown that the dimer and monomer radical anions of acetonitrile are produced and stabilized in Crystal I and Crystal II, respectively.[7] The optical absorption spectrum of the dimer radical anion in a polycrystalline sample has two bands with λ_{max} at 510 nm[8,9] and 310 nm[9] whereas the corresponding spectrum of the monomer radical anion has only one clearly defined band with λ_{max} at 430 nm.[9] In similar low-temperature irradiation studies, the dimer

radical anion of succinonitrile was identified in both crystalline phases.[10]
Its powder esr spectrum is identical to that of the acetonitrile dimer
radical anion[11] and λ_{max} for the optical absorption is located at 540 nm.[10]

Succinonitrile differs from other simple organic cyanides in having
a relatively high mp (331°K). Also, the solid phase above 233°K (Crystal
I) is a transparent plastic crystal in which the rotational motion of the
individual molecules is more characteristic of a liquid than of a solid.[12]
It was thought that the physical properties of this plastic crystal[13] which
are intermediate between those of a liquid and a solid might favor the
detection by pulse radiolysis of a succinonitrile radical anion (or solvated
electron) at room temperature. This finding would be of particular interest
in view of the close resemblance between the γ-irradiation results for
acetonitrile and succinonitrile at low temperature, and the absence of
any significant information about the reactions of electrons with alkyl
cyanides in the liquid phase.[14]

Experimental Section

Materials and Preparation of Samples. Succinonitrile (Matheson
Coleman and Bell) was distilled at reduced pressure and stored under
vacuum in breakseals. The material was either redistilled in vacuo or
transferred manually into the sample cell, and subsequently degassed before
the cell was sealed. The pulse radiolysis results were the same regardless
of the method of sample preparation. Tetracyanoethylene (TCNE), obtained
as a White Label grade from Eastman Organic Chemicals, was used as received.
Samples of succinonitrile containing a weighed amount of TCNE (~1 mole %)

were prepared by placing both compounds in a cell after which the mixture was degassed by several cool-pump-melt cycles. The resulting solid solution was quite transparent, suggesting that the TCNE was uniformly incorporated.

Irradiation Cells. The Suprasil cells used in this investigation were the same as those which have been employed in this laboratory for low-temperature optical studies.[9] The flat portion of the cell containing the sample is rectangular (1.2 cm width x 1.5 cm height) with a path length of 0.1 cm, and is fused to the quartz section of an 8 mm quartz-to-pyrex graded seal.

Pulse Radiolysis. The irradiation cell, mounted on an aluminum plate, was inserted into the sample holder of the apparatus.[15,16] A 1.2 cm aperture in the plate accommodates the four passes of the analytical light which are collinear with the electron beam, thereby giving a total optical path length of 0.4 cm. A high pressure Hg-Xe arc (Hanovia Model 901B-1) was used as the source of analytical light. This lamp was pulsed to an intensity approximately fifty times that obtainable in dc operation to minimize the correction for emission from the Suprasil cell during the first μsec after the pulse. The lamp was not pulsed in experiments which did not require μsec time resolution. To minimize the photolytic effects of the analytical light, a Corning C.S. 0-51 filter, which does not transmit below 400 nm, was placed between the lamp and the sample. In studying the decay of TCNE⁻, Corning filters C.S. 3-73 and C.S. 1-56 were used to transmit a narrow band centered at 440 nm.

Through the use of the McPherson Model 216 polychromator and a double slit mechanism, it was possible to monitor the absorption at two wavelengths simultaneously. For 3 mm slits and a grating with 1200 lines/mm, the bandwidth of the light beam reaching the photomultipliers is 2 nm.

The calculation of the dose received by the sample was based on measurements of the energy absorbed in a thin aluminum calorimeter placed at the sample position.[16] After correcting for the depth-dose effect[16] and the estimated ratio (1.20 ± 0.10) of the mass stopping powers of succinonitrile and aluminum,[17] the average dose per pulse was calculated to be 9.0×10^{18} ev g^{-1} (1.44×10^{5} rad). The dose per pulse has been shown to be reproducible within 5% from pulse to pulse.

Results

Initial experiments revealed an absorption in the 350-600 nm region after the pulse. Examination of the oscillograms showed that the absorption was composed of two components, a transient absorption with a μsec lifetime and a much longer-lived absorption which persisted for at least 5 min and will henceforth be referred to as the permanent absorption. In addition, by pulsing the Febetron with no analytical light, it was found that the oscilloscope trace was further complicated by light emission of ca. 1 μsec duration. This emission was also observed from an empty irradiation cell indicating that it originates from the Suprasil windows through which the electron beam penetrates.

Figure 1 shows a typical oscillogram with the monochromator set at 400 nm. The upper trace is the composite signal and the lower trace is the emission signal recorded in the subsequent pulse on the same transmission

scale. The net absorption signal was obtained by subtraction. In order to correct for the permanent absorption, it was assumed that this signal reached its maximum value at the same time (0.2 μsec) as that of the transient signal, and then remained constant. The validity of this assumption was verified in subsequent experiments on solid solutions of TCNE in succinonitrile, as will be discussed later. Accordingly, the absorbance of the transient was evaluated as the difference between the net and permanent absorbances.

Since repetitive pulsing of the same sample led to a marked decrease in the signal intensity of the transient, the spectrum was derived by the simultaneous recording of the absorption signals at two wavelengths, one of which was fixed at 475 nm to serve as a reference, and the other was varied from pulse to pulse to cover the range from 350 to 550 nm. A typical oscillogram obtained by using this technique is shown in Figure 2. The traces A and B refer to the absorption and emission, respectively, at 475 nm, and the traces C and D are the corresponding signals at 500 nm. It is evident that the transient species is completely formed within 0.2 μsec after the beginning of the pulse, and optical densities were measured after this time. By taking the ratio of the optical densities at the monitoring wavelength and 475 nm from each oscillogram, the spectrum of the transient was obtained at 0.2 μsec and normalized to the optical density at 475 nm in the first pulse. This spectrum is shown in Figure 3 and λ_{max} is in the region of 450 nm. The $\underline{G} \epsilon_{max}$ product is 8.2 x 10^3 (molec/100 eV) $\underline{M}^{-1}$ cm^{-1}.

Evidence that the transient spectrum results from only one species is provided by the decay kinetics. Excellent first-order plots were obtained at all wavelengths between 350 and 550 nm. Measurements were made at intervals of 25 nm. The first-order rate constants were in good agreement and gave an average value of $3.0 \pm 0.6 \times 10^6$ sec^{-1} over this range. It was also clearly demonstrated that the decay of the transient species proceeds by a thermal and not a photochemical reaction, for reducing the intensity of the incident analytical light by a factor of 2.5 did not alter the first-order rate constant.

In an attempt to establish the nature of the transient species, experiments were carried out with solutions of TCNE which is known to be an excellent electron scavenger. The monochromator was set at 550 nm where TCNE$^-$ does not absorb but where the transient species shows a significant absorption (Figure 3). A comparison of the results for pure succinonitrile and a TCNE solution (Figure 4) shows that the presence of the TCNE eliminates the transient but has no effect on the appearance of the permanent absorption. It is from this experiment, where no transient is observed, that the permanent absorption signal is seen to grow in during the first 0.2 µsec after the pulse and to maintain a constant value for the subsequent 2 µsec. This justifies the previous assumption that the permanent absorption remains unchanged during the decay of the transient in pure succinonitrile.

The identification of TCNE$^-$ in the above experiment proved to be a relatively simple task. A strong long-lived absorption below 500 nm was

detected on the oscilloscope and _ca_. 1 min after the pulse, the sample was removed from the apparatus and plunged into liquid nitrogen. The optical spectrum recorded at 77°K, where there was no decay, is shown in Figure 5, and the positions of the well-resolved peaks correspond to those reported[18,19] for TCNE⁻ . In the light of this result, a detailed examination of the decay of TCNE⁻ at room temperature was made by following the absorption peak at 438 nm. Although some decay occurred in the msec region, most of the absorption disappeared according to first order kinetics with $t_{1/2}$ = 9.3 min.

As indicated by the oscilloscope traces (_cf_. Figures 1 and 4), the rapidly-induced permanent absorption in succinonitrile is more intense at shorter wavelengths. This absorption increases only slightly on standing at room temperature for several min after the pulse, and its uv spectrum recorded with a conventional spectrophotometer exhibits a sharp rise to shorter wavelengths with a well-defined shoulder at 245 nm. A similar feature is observed at 265 nm in the spectrum of γ-irradiated succinonitrile Crystal II after photobleaching at 77°K.

Discussion

As a result of the TCNE experiments, it has been clearly established that the transient species in succinonitrile originates by electron capture. Its absorption spectrum (λ_{max} = 450 nm) differs from that of the dimer radical anion (λ_{max} = 540 nm) produced at low temperature[10] but is remarkably similar to the spectra of the monomer radical anions of acetonitrile[9] and adiponitrile[20] for which λ_{max} is between 430 and 440 nm. On the basis

of this correlation, and in view of the suggestion[21] that a solvated electron in acetonitrile would have an absorption peak in the near infrared, the transient spectrum is assigned to a succinonitrile monomer radical anion, although the choice between the monomer and dimer radical anion cannot be made with absolute certainty owing to the broad nature of the absorption bands. Since the monomer is likely to be the precursor of the dimer, it is possible that the conditions favoring the formation of the dimer may not exist at room temperature. In this connection, the rotational motion characteristic of succinonitrile at room temperature[13a] could prevent the precise alignment of the cyanide groups required for dimer formation.[7]

The short lifetime ($t_{1/2}$ = 0.23 μsec) of the transient species is most likely to be determined either by ionic recombination or by dissociation. The other possibility that the species disappears by reaction with neighboring molecules in the lattice is considered improbable in view of the well-known stability of many radical anions in aprotic media.[14a] Since the decay of $TCNE^-$ occurs on a much longer timescale than that of the transient, this would appear to exclude ionic recombination as a mechanism for the disappearance of the transient. Hence, the most reasonable path is suggested to be simple dissociation of the monomer radical anion to give CN^- and $\cdot CH_2CH_2CN$. This is consistent with the instability of isostructural molecules such as HCN^- [22] and $CH_3\overset{\cdot}{C}O$ [23] at elevated temperatures. Confirmation of the dissociation reaction by direct observation of the $\cdot CH_2CH_2CN$ would have been desirable but was prevented by the intense permanent absorption in the ultraviolet.

The formation of the permanent absorber is unaffected by the incorp-oration of TCNE so it can be safely assumed that it does not arise from a reaction involving electrons liberated in the ionization process. Its optical spectrum showing a high intensity in the uv and a long tail in the visible region is indicative of a highly conjugated structure, as would be produced by the polymerization of $-C\equiv N$ groups. From the fact that the yield of the transient species diminished on repeated pulsing, it is conceivable that the permanent absorber acts as a competitive electron scavenger.

Based on the value of $\epsilon = 7.1 \times 10^3 \ \underline{M}^{-1} \ cm^{-1}$ for TCNE$\bar{}$ at 435 nm,[18] $\underline{G}$(TCNE$\bar{}$) is 4.0 which demonstrates very efficient trapping of electrons. Unfortunately, an estimate of the $\underline{G}$ value for the transient radical anion cannot be made since there has been no independent determination of ϵ_{max} for species of this type. However, the $\underline{G} \ \epsilon_{max}$ product of 8.2×10^3 (molec/100 eV) $\underline{M}^{-1} \ cm^{-1}$ in this pulse radiolysis study is comparable to the range of values $(4 \times 10^3 - 1 \times 10^4)$[9a,10] obtained for monomer and dimer radical anions of nitriles at 77°K, implying that electron capture is as efficient in succinonitrile at room temperature as it is at low temperature, although the thermal stability of the ion is much less in the former case. As a concluding remark, the failure to observe radical anions in the pulse radiolysis of pure liquid acetonitrile[6] could perhaps be attributed to the greater instability of these ions at elevated temperatures, particularly in the absence of an ordered lattice.

REFERENCES

(1) (a) Kinetics of Ionic Processes in the Radiolysis of Liquids. VI;[1b]
(b) Part V: R. B. Taylor and F. Williams, $\underline{J}$. $\underline{Amer}$. $\underline{Chem}$. $\underline{Soc}$., $\underset{\sim}{91}$, 3728 (1969).

(2) This research was supported by the U.S. Atomic Energy Commission at the Oak Ridge National Laboratory operated under Contract with the Union Carbide Company and at The University of Tennessee under Contract No. AT-(40-1)-2968; this is AEC Document No. ORO-2968-71.

(3) (a) University of Tennessee: undergraduate on leave from New College, Sarasota, Fl. 33578;
(b) Oak Ridge National Laboratory;
(c) University of Tennessee.

(4) R. A. Holroyd in "Fundamental Processes in Radiation Chemistry," P. Ausloos, Ed., Wiley, New York, N.Y., 1968, Chapter 7, p 413.

(5) A. Singh, H. D. Gesser, and A. R. Scott, $\underline{Chem}$. $\underline{Phys}$. $\underline{Lett}$., $\underset{\sim}{2}$, 271 (1968).

(6) E. Hayon, $\underline{J}$. $\underline{Chem}$. $\underline{Phys}$., $\underset{\sim}{53}$, 2353 (1970).

(7) E. D. Sprague, K. Takeda, and F. Williams, $\underline{Chem}$. $\underline{Phys}$. $\underline{Lett}$., $\underset{\sim}{10}$, 299 (1971).

(8) L. Holloman, E. D. Sprague, and F. Williams, $\underline{J}$. $\underline{Amer}$. $\underline{Chem}$. $\underline{Soc}$., $\underset{\sim}{92}$, 429 (1970).

(9) (a) L. Holloman, M. S. Thesis, The University of Tennessee, 1970;
(b) E. D. Sprague, Ph.D. Thesis, The University of Tennessee 1971.

(10) A. Campion and F. Williams, $\underline{J}$. $\underline{Chem}$. $\underline{Phys}$., $\underset{\sim}{54}$, 4510 (1971).

(11) M. A. Bonin, K. Takeda, and F. Williams, $\underline{ibid}$., $\underset{\sim}{50}$, 5423 (1969).

(12) C. A. Wulff and E. F. Westrum, Jr., $\underline{J}$. $\underline{Phys}$. $\underline{Chem}$., $\underset{\sim}{67}$, 2376 (1963).

(13) (a) J. G. Powles, A. Begum, and M. O. Norris, $\underline{Mol}$. $\underline{Phys}$., $\underset{\sim}{17}$, 489 (1969); (b) H. M. Hawthorne and J. N. Sherwood, $\underline{Trans}$. $\underline{Faraday}$ $\underline{Soc}$., $\underset{\sim}{66}$, 1792 (1970).

(14) Reviews of solvated electrons and radical ions are given in the following works: (a) M. Szwarc, "Carbanions, Living Polymers, and Electron Transfer Processes," Wiley, New York, N.Y., 1968, Chapter VI, p 297; (b) "Radical Ions" (eds. E. T. Kaiser and L. Kevan), Wiley, New York, N.Y., 1968.

(15) C. J. Hochanadel, J. A. Ghormley, and J. W. Boyle, $\underline{J}$. $\underline{Chem}$. $\underline{Phys}$., $\underset{\sim}{48}$, 2416 (1968).

(16) J. A. Ghormley, C. J. Hochanadel, and J. W. Boyle, _ibid._, 50, 419 (1969).

(17) _cf_. J. W. T. Spinks and R. J. Woods, "Introduction to Radiation Chemistry," Wiley, New York, N.Y., 1964, p 92.

(18) O. W. Webster, W. Mahler, and R. E. Benson, J. Amer. Chem. Soc., 84, 3678 (1962).

(19) M. R. Ronayne, J. P. Guarino, and W. H. Hamill, J. Amer. Chem. Soc., 84, 4230 (1962).

(20) A. Campion, K. Takahashi, and F. Williams, unpublished work.

(21) R. J. Egland and M. C. R. Symons, J. Chem. Soc. (A), 1326 (1970).

(22) F. J. Adrian, E. L. Cochran, V. A. Bowers, and B. C. Weatherley, Phys. Rev., 177, 129 (1969).

(23) J. E. Bennett and B. Mile, Trans. Faraday Soc., 67, 1587 (1971).

CAPTIONS TO FIGURES

Figure 1. Oscillogram showing the absorption in pure succinonitrile at 400 nm. The upper trace is the composite absorption signal, and the lower trace shows the emission from the sample cell.

Figure 2. Oscillogram showing absorption and emission at 475 nm (traces A and B) and 500 nm (traces C and D).

Figure 3. Optical spectrum of the transient radical anion produced by pulse radiolysis of succinonitrile at room temperature. Optical densities were measured at 0.2 μsec after the beginning of the pulse.

Figure 4. Oscillograms showing absorption and emission at 550 nm. The traces in the upper photograph are for pure succinonitrile and those in the lower photograph are for succinonitrile doped with 1 mole % tetracyanoethylene.

Figure 5. Optical absorption spectrum of the tetracyanoethylene radical anion in polycrystalline succinonitrile at 77°K. The radical anion was produced by pulse radiolysis of succinonitrile containing 1 mole % tetracyanoethylene at room temperature and then stabilized at 77°K.
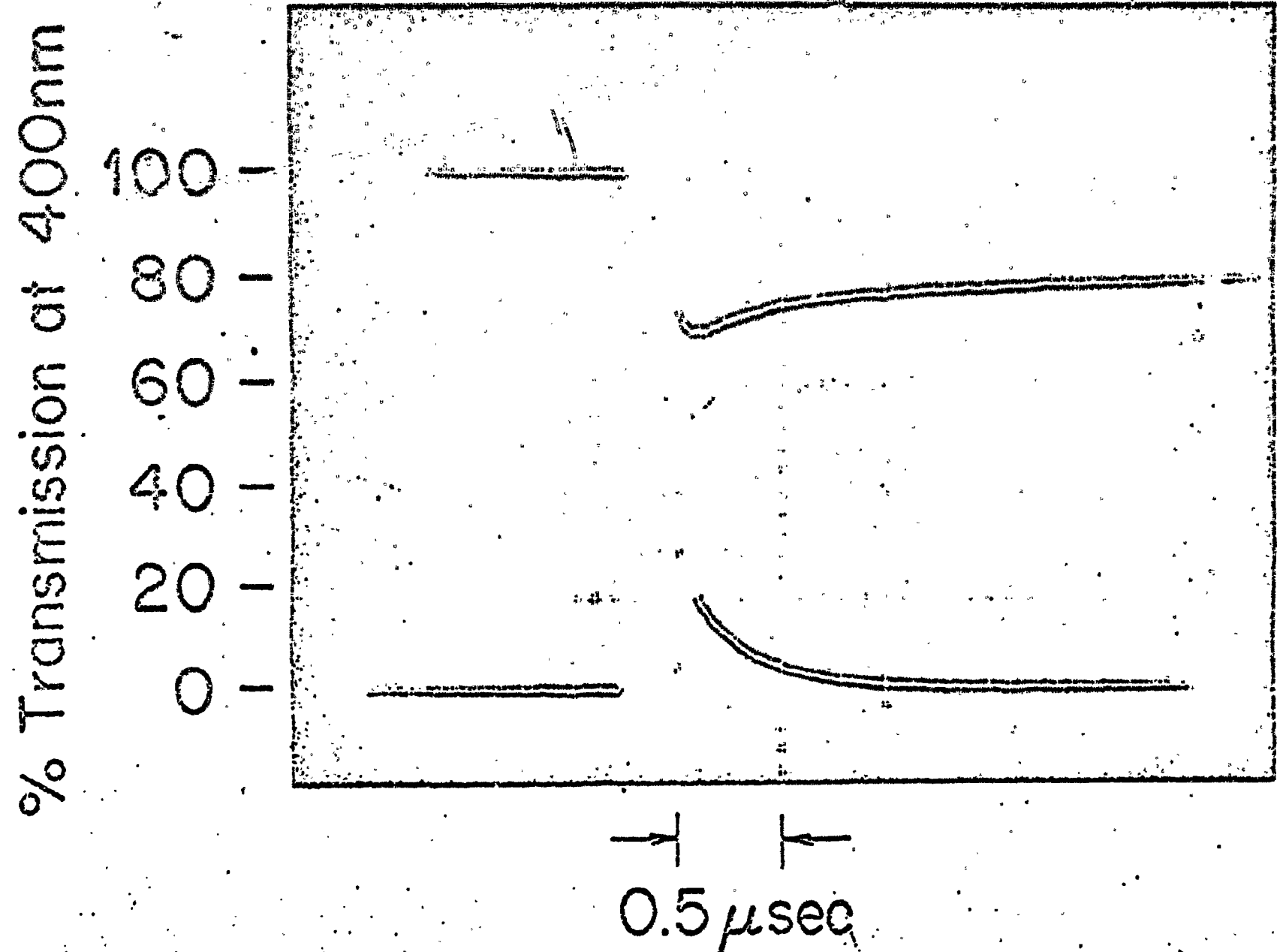
Figure 1   Campion, Ghormley, and Williams

% Transmission at 475nm

% Transmission at 500nm
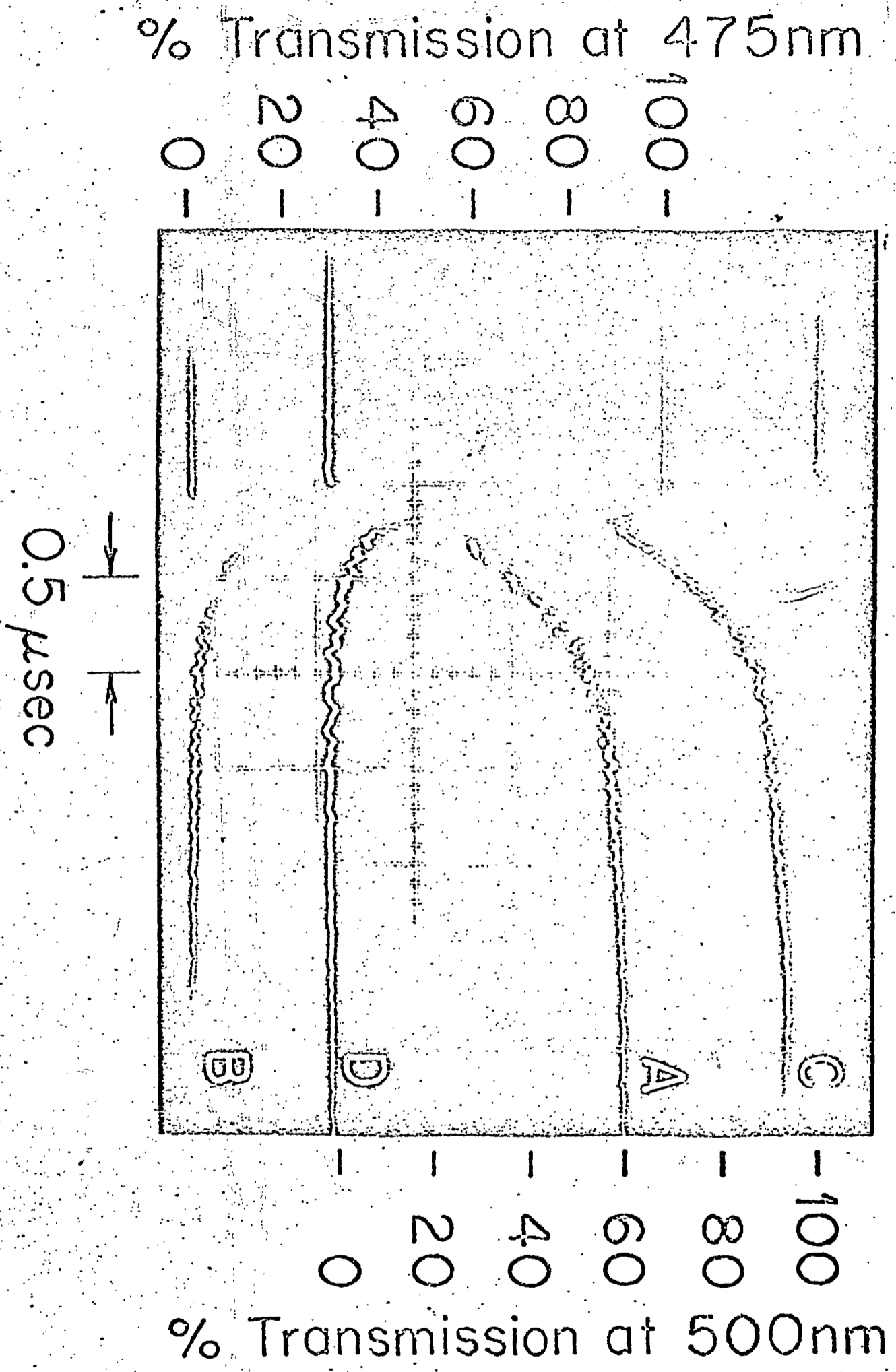
0.5 μsec

Figure 2 — Campion, Ghormley, and Williams
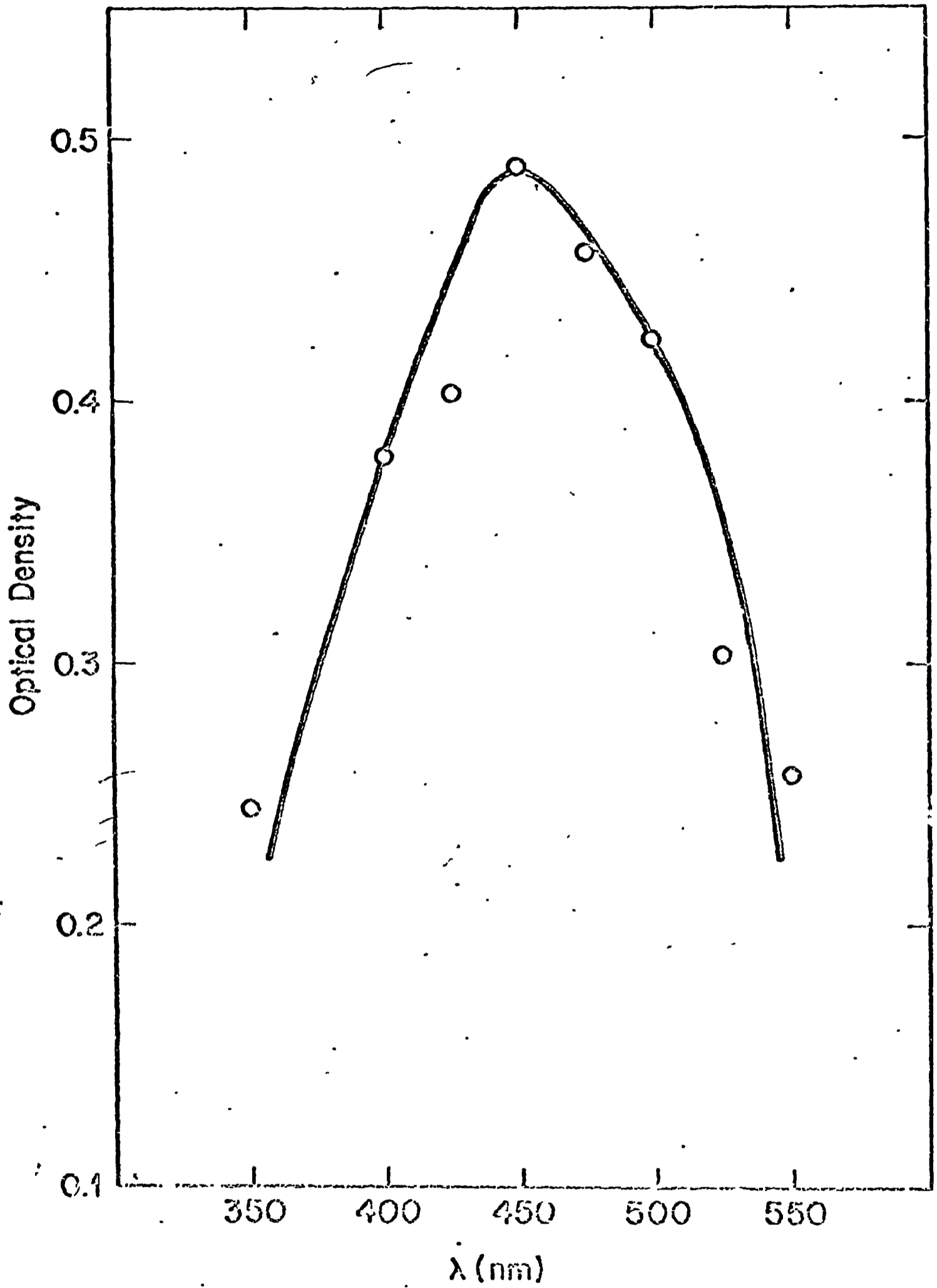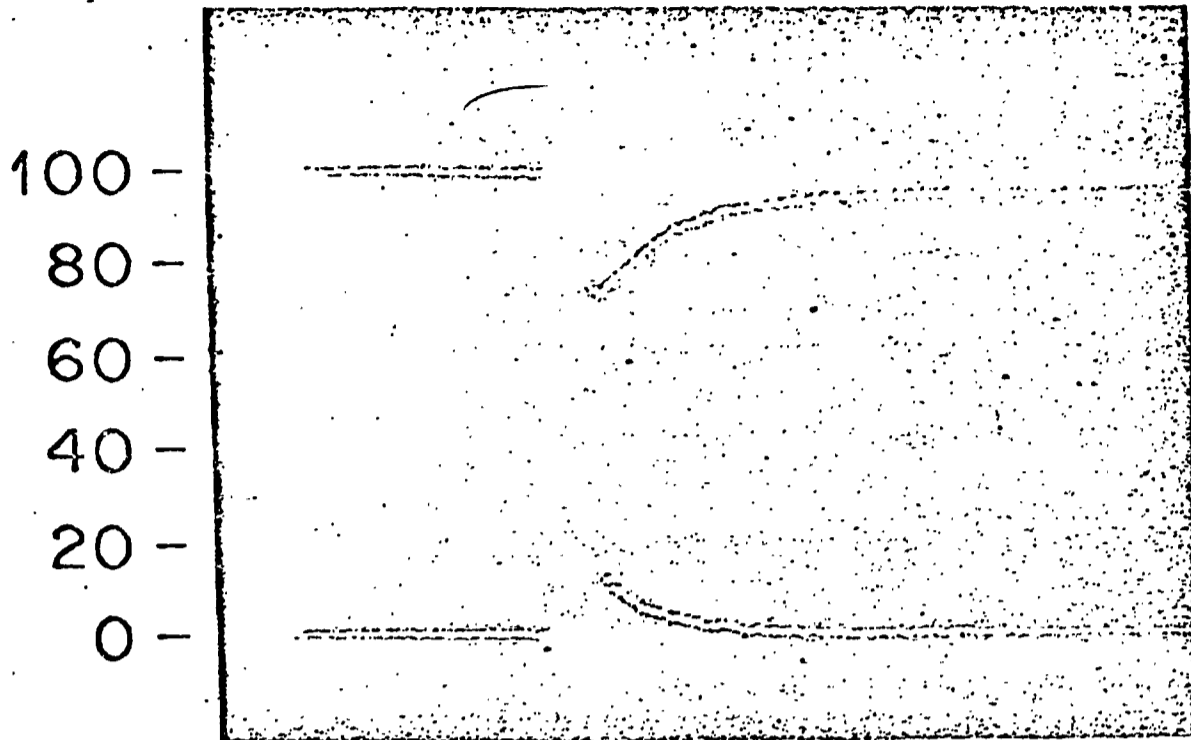
Figure 3   Campion, Ghormley, and Williams
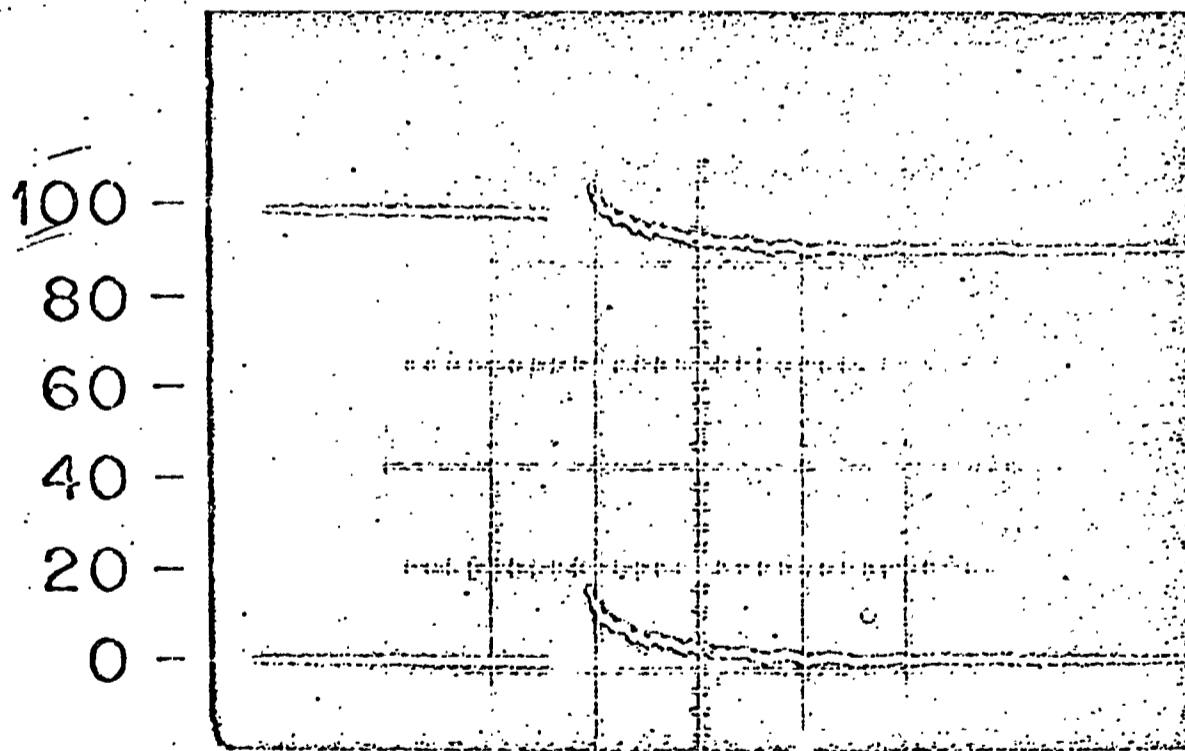
Figure 4   Campion, Ghormley, and Williams
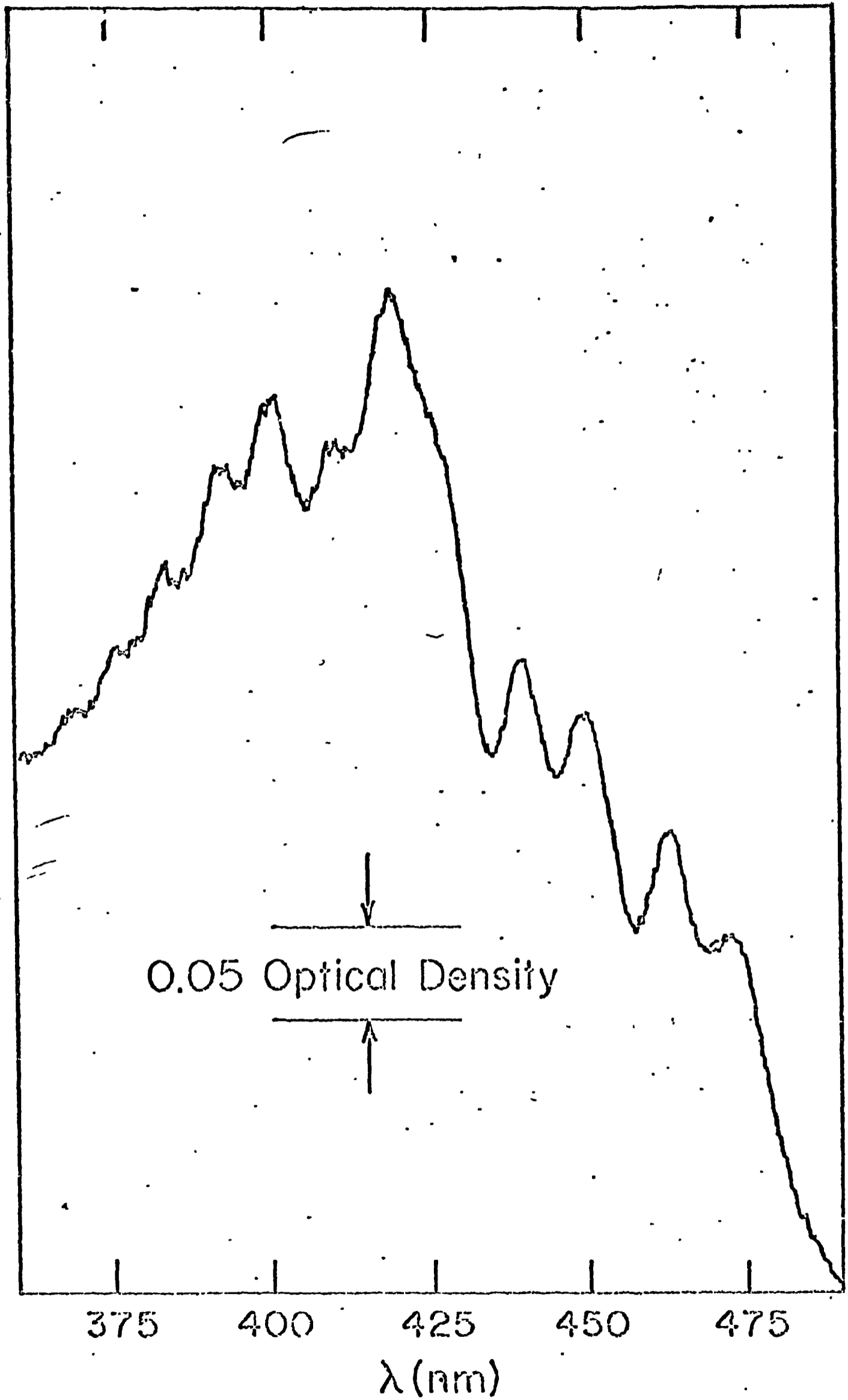
0.05 Optical Density

λ(nm)

Figure 5   Campion, Chormley, and Williams

An Investigation of the Structure of the Hydrated Electron based on Unpaired

Electron Densities Calculated by the INDO Method[1]

by Carolyn M. L. Kerr[*2] and Ffrancon Williams

Department of Chemistry, University of Tennessee, Knoxville, Tennessee 37916

(Received   )

Spin density distributions have been calculated for a number of possible

structures for the hydrated electron, and the total spin density associated

with the hydrogen atoms compared with the value derived from esr experiments.

Although the agreement with experiment is not close, the best results are

obtained for a planar dimeric structure containing two central hydrogens

close to one another. The structure of the hydrated electron may incorporate

symmetrically placed units of this type.

Editorial correspondence and proofs should be sent to:

    Ffrancon Williams
    Department of Chemistry
    University of Tennessee
    Knoxville, Tennessee 37916

1. Introduction

In this study the INDO method[3] has been employed to investigate the structure of the hydrated electron using a comparison of the experimental and theoretical spin densities on the hydrogen nuclei as a criterion of structural validity. This approach is used in preference to the conventional one of minimizing the energy of the system with respect to geometrical parameters for two reasons. First, the spin density distribution for a paramagnetic species is generally very sensitive to the molecular structure, and the INDO method has been shown to yield isotropic hyperfine coupling constants in good agreement with experiment for a wide variety of both σ and π radicals whose geometries can be reasonably well defined.[3c] The agreement is generally better for hydrogen than for second row elements. Secondly, the INDO method is not always reliable for predicting equilibrium geometries based on energy minimization. This is hardly surprising since the parameterization was intended to yield charge densities and spin densities rather than properties dependent on the molecular energies.[4]

The use of a completely molecular description instead of the familiar cavity or polaron models[5] of the hydrated electron stems from recent work in this laboratory on electron excess centers in acetonitrile[6] and sulfuryl chloride.[7] In acetonitrile, γ-irradiation yields either the monomer or dimer radical anion depending upon the crystalline phase. The monomer radical anion is a typical σ-radical with appreciable spin density in the 2s orbital of the nitrile carbon due to the bending of the molecule. On

the other hand, the spin density distribution in the dimer radical anion
indicates the unpaired electron is associated with two equivalent and essent-
ially linear molecules, with most of the spin density in the p orbitals
on nitrogen. According to a simple MO description, the dimer radical anion
can be considered as a radical anion complex in which the unpaired electron
occupies a supramolecular bonding orbital derived from the antibonding orbitals
of two separate molecules. The radical anion of sulfuryl chloride can be
described similarly, and in this case the molecular orbitals involved are
essentially the lowest antibonding orbitals of adjacent sulfur dioxide and
chlorine molecules.

In certain respects, the properties of the dimer radical anion of
acetonitrile resemble those of trapped electrons in glasses. In particular,
the esr signals of both these species saturate readily with microwave power
and the optical absorption spectra are characteristically broad. These
similarities suggest that in the case of trapped or solvated electrons, the
excess electron may be confined to the orbitals of two or more solvent
molecules rather than to an interstitial cavity. According, the hydrated
electron can be formally represented as $(H_2O)_{\underline{n}}^{-}$.

The esr spectrum of the trapped electron in aqueous solids is generally
a broad singlet but hyperfine structure has been resolved in two instances.[8,9]
Both in crystalline ice co-deposited with alkali metals[8] and, more recently,
in a γ-irradiated alkaline glass,[9] the spectrum was shown to consist of
an odd multiplet with a splitting of approximately 5 G. From these results,
it has been suggested that the trapped electron interacts with either

four[8] or six[9] protons. In any event, the existence of resolved hyperfine features certainly points to a well-defined molecular structure for $(H_2O)_n^-$ rather than to a disordered cage of water molecules surrounding a trapped electron. A lineshape analysis[10] on the unresolved spectrum also indicates that the hyperfine interaction is limited to a relatively small number (8±2) of protons. If eight protons can be considered an upper limit, the observed hfs of 5 G as compared to the value of ca. 500 G for the isolated H• atom indicates a spin density of ca. 1% and hence a total for the complex of 8% or less. The aim of the present work has been to seek structures of $(H_2O)_n^-$ for which the calculated spin density distribution approximates most closely to this experimental result.

2. Calculations

The INDO method employs a valence orbital basis set which in this case consists of the 1s orbitals on hydrogen and 2s and 2p orbitals on oxygen. The calculations yield the spin density distribution of the excess electron over the valence shell orbitals of the water molecules in the complex.

Bond orders between two atoms were calculated as the sum of all off-diagonal elements involving the atoms in the charge density matrix. While the numerical values obtained have no absolute significance, comparison of bond orders in a closed shell species and in the negatively charged open shell species with the same geometry can be used to determine the bond-breaking or bond-forming effect resulting from the addition of an electron.

3. Results

The results of calculations on the monomer, H_2O^-, are presented first. For this species, the OH bond length was varied from 0.08 to 0.19 nm in increments of 0.01 nm, and the HOH angle from 60° to 180° in increments of 10°. The corresponding values for the neutral molecule are 0.096 nm and 105°.[11] Positive spin density is always obtained in the s orbitals of both hydrogen and oxygen. There is also considerable spin density in the oxygen p_x and p_y orbitals, but none in the p_z orbital (see Figure 1 (a)). The spin densities in the p_x and p_y orbitals are always of opposite sign, and increase monotonically with the bond length. The positive spin density is associated with the p_y orbital for OH distances of 0.08 - 0.14 nm and for HOH angles of 60-90°, and with the p_x orbital for all other geometries. The total spin density on hydrogen, ρ_H^T, where this quantity is defined generally for multimeric species as

$$\rho_H^T = \sum_{all\ H} |\rho_H| \quad ,$$

varies both with bond angle and bond length as shown in Figure 2. For the shorter bond lengths, minima occur in the curves for angles of 100 to 110°, but there is no corresponding optimum bond length, ρ_H^T increasing regularly as the OH distance is increased. The O-H bond order decreases steadily with increasing bond length, and for bond lengths up to 0.14 nm, it has a value which is about 0.7 times that of the neutral molecule

with the same geometry. For higher bond lengths, the bond orders for H_2O^- and H_2O are both small. These factors and the high negative spin densities observed in the oxygen p orbitals suggest that the large values of ρ_H^T and their variation with bond length reflect a progressive breakdown in the OH bonding.

The large ρ_H^T found for H_2O^- definitely excludes this as the structure of the hydrated electron. However, by analogy with acetonitrile where there are profound differences between the spin density distributions and structures of monomer and dimer radical anion, this does not rule out the possibility that suitable combinations of H_2O molecules could yield values of ρ_H^T in closer accord with experiment. Based on this, our approach has involved the determination of ρ_H^T for multimeric species $(H_2O)_{\underline{n}}^-$. Since the values of ρ_H^T for the monomer are extremely large, we have investigated various geometrical arrangements of molecules in $(H_2O)_{\underline{n}}^-$ complexes to determine which configurations lead to a decrease in ρ_H^T.

Calculations have been done on a variety of different dimeric structures. The first set of structures are shown in Figure 1, (b)-(f). The distinguishing feature of these is that the oxygen p orbitals are aligned so that a strong overlap is possible. It has been shown previously[7] that an excess electron can be effectively shared between two molecules through positive overlap of antibonding orbitals from the separate molecules. An additional consideration in the present case is that bonding between the H_2O molecules through the oxygen p orbitals might redistribute the spin density in favor of these orbitals, thereby decreasing ρ_H^T.

For any particular structure, equivalent H_2O geometries were always employed. The OH bond length, the HOH angle, and $\underline{d}$, the distance apart of the oxygen atoms, were varied independently over the ranges 0.09 – 0.12 nm, 90 – 135°, and 0.16 – 0.24 nm, respectively. The results showed that in structure (b), there appeared to be no delocalization and the distribution was essentially that of the H_2O^- monomer and a neutral H_2O molecule for all configurations; in all the other structures, the unpaired electron was shared equally between the two molecules. For structures (c) and (d), there was no reduction in ρ_H^T whereas a reduction was found for structures (e) and (f), this being larger in the case of the former for all configurations. A number of structures intermediate between (e) and (f) were generated by allowing the hydrogen atoms of the upper molecule to range over the surface of a hemisphere, as shown in Figure 1(e). For all of these, ρ_H^T was found to be greater than the value for structure (e), suggesting that parallel alignment of the p orbitals is a contributing factor in reducing ρ_H^T.

The calculations were extended to trimer and tetramer for model (e). Although there were some irregularities, in general ρ_H^T decreased monotonically in going from monomer to tetramer and the largest decreases were observed for OH bond lengths of 0.11 – 0.12 nm, an HOH angle of 105°, and $\underline{d}$ = 0.18 – 0.20 nm. The results are summarized in Table I. For these geometries, the spin density on oxygen is largely in the $p_{\underline{x}}$ orbital with small negative contributions in the $p_{\underline{y}}$ and $p_{\underline{z}}$ orbitals, as shown in

Table II. It can also be seen from the data given in this Table that the overall distribution of the spin density in an individual molecule is not greatly altered between monomer and tetramer.

The models discussed above are somewhat unrealistic. Since the microstructure of an aqueous solid is controlled by hydrogen bonding, models in which molecules are linked by hydrogen bonding should also be considered. Although other configurations have been observed, hydrogen bonded systems generally involve linear or nearly linear O------H——O units. A simple dimer incorporating this feature is shown in Figure 3(a), the O------H——O line making an approximately tetrahedral angle with the O-H bonds of molecule 2. Calculations were performed for the same range of bond lengths and bond angles as previously and oxygen-oxygen distances of 0.24 to 0.30 nm (the corresponding distance in ice is 0.276 nm[11]). In all these cases, the unpaired electron was effectively localized on one molecule. Small rotations (up to 30°) of molecule 2 about the three coordinate axes (see Figure 1(a)) hardly affected the delocalization or the value of ρ_H^T, indicating that structures derived from a hydrogen-bonded fragment are unfavorable.

Further calculations were then carried out for an OH bond length of 0.11 nm, an HOH bond angle of 105°, an oxygen-oxygen distance of 0.27 nm, and configurations such that the position of molecule 1 and the linearity of the O------H——O unit were retained and the hydrogen

atoms of molecule $\underset{\sim}{2}$ were rotated over the surface of a sphere. Over

a small range of configurations, both delocalization and a decrease in

ρ_H^T were observed. Once the configuration yielding the minimum value

of ρ_H^T had been determined, ρ_H^T was minimized with respect to the bond

length, bond angle, and oxygen-oxygen distance, these parameters being

varied over the ranges 0.09 to 0.12 nm, 90 to 135°, and 0.25 to 0.35 nm,

respectively. The lowest value of ρ_H^T was found for the configuration

shown in Figure 3 (b) with an OH bond length of 0.12 nm, a bond angle

of 105°, and an oxygen-oxygen distance of 0.31 nm. The spin density

distributions for this structure and for the monomer with the same molecular

geometry are shown in Table III. A further limited number of calculations

were performed with the above molecular geometry, but varying the orient-

ations of both molecules and the distance between them. Spin densities

close to the values obtained for the dimer in Figure 3(b) were found for

dimers symmetrical about the oxygen-oxygen axis and with hydrogen-hydrogen

distances of 0.08 to 0.09 nm. Slightly higher spin densities were obtained

for symmetrical dimers containing linear O——H——————H——O units. The

minimum values of ρ_H^T found for these structures are listed (Table III) with

the associated structural parameters and spin densities.

From the data given in Table III, it can be seen that the distribution

is substantially different for monomer and dimer, in contrast to the results

obtained for model (e). There is a marked shift of both spin density and

charge density from hydrogen to oxygen in the dimer relative to the monomer.

A further point to note is that the spin densities in all orbitals of the

dimers in Table III are zero or positive.

The proximity of the central hydrogen atoms appears to be an important feature of these structures. Low values of ρ_H^T were only observed for hydrogen-hydrogen distances in the range 0.07 - 0.10 nm, and these were associated with bond orders between the hydrogen atoms of 0.5 - 0.7. The bond orders in the corresponding neutral molecule dimer are almost a factor of two less than this, and the values for isolated hydrogen molecules are 1.0.

4. Discussion

In this paper we have examined the possibilities for determining the structure of the hydrated electron by comparison of theoretical and experimental unpaired electron densities. Although the investigations of the various structures are not exhaustive, they are reasonably detailed and lead to two general conclusions. Firstly, dimers with certain configurations can yield values of ρ_H^T substantially less than that for the monomer with the same molecular geometry. Secondly, for a dimer structure which was shown to yield a reduced ρ_H^T, then further reduction was obtained by increasing the number of molecules in the complex.

It is interesting that the optimum dimer model on the basis of spin densities is structurally similar to others proposed on other grounds. The dimer structure suggested by Raff and Pohl[12] consists essentially of an H_2^+ fragment perturbed by two OH$^-$ ions. A degree of bonding is thus implied between the central hydrogens. This model yields a value for the optical excitation energy in good agreement with experiment. Webster and

his co-workers[13] have investigated a similar model, _viz_. a planar dimer containing a linear O——H------H——O unit, using two different molecular orbital methods. In both cases, structures corresponding to the minimum energy give excitation energies close to the experimental value. However, the predicted hydrogen-hydrogen separations (0.12 nm for the INDO and 0.15 nm for the extended Hückel method) are somewhat larger than the range (0.07-0.10 nm) found in the present work.

While the dimer shown in Figure 3(b) clearly does not represent the complete structure of the hydrated electron, it has several favorable features which suggest that the complete structure may incorporate units of this type. Moreover, if a larger even number of molecules, _i.e._ four or six, is used, symmetrical structures can be constructed which contain four or more equivalent protons as required by the esr results,[8-10] and calculations are currently in progress for these systems.

REFERENCES

(1) This research was supported by the U.S. Atomic Energy Commission under Contract No. AT-(40-1)-2968, and this is AEC Document No. ORO-2968-75.

(2) Author to whom correspondence should be addressed at the Department of Chemistry, The University, Southhampton, S09 5NH, Hampshire, England.

(3) (a) J. A. Pople and D. L. Beveridge, "Approximate Molecular Orbital Theory," McGraw-Hill Book Co., New York, N.Y., 1970; (b) Program 141, Quantum Chemistry Program Exchange, Department of Chemistry, Indiana University, Bloomington, Ind. 47401. Computations were carried out on an IBM System 360/65 digital computer; (c) J. A. Pople, D. L. Beveridge, and P. A. Dobosh, $\underline{J}$. $\underline{Amer}$. $\underline{Chem}$. $\underline{Soc}$., 90, 4201 (1968).

(4) J. N. Murrell and A. J. Harget, "Semi-empirical SCF Molecular Orbital Theory of Molecules," Wiley-Interscience, New York, N.Y., 1972, p 57.

(5) J. Jortner in "Actions Chimiques et Biologiques des Radiations," M. Haissinsky, Ed., Volume 14, Masson et Cie., Paris, 1970.

(6) E. D. Sprague, K. Takeda, and F. Williams, $\underline{Chem}$. $\underline{Phys}$. $\underline{Lett}$., 10, 299 (1971).

(7) (a) C. M. L. Kerr and F. Williams, $\underline{J}$. $\underline{Amer}$. $\underline{Chem}$. $\underline{Soc}$., 93, 2805 (1971); (b) C. M. L. Kerr and F. Williams, $\underline{ibid}$., 94, 0000 (1972).

(8) J. E. Bennett, B. Mile, and A. Thomas, $\underline{J}$. $\underline{Chem}$. $\underline{Soc}$., A, 1393 (1967); J. E. Bennett, B. Mile, and A. Thomas, $\underline{ibid}$., 1502 (1969).

(9) K. Ohno, I. Takemura, and J. Sohma, $\underline{J}$. $\underline{Chem}$. $\underline{Phys}$., 56, 1202 (1972).

(10) B. G. Ershov and A. K. Pikaev, $\underline{Radiation}$ $\underline{Res}$. $\underline{Rev}$., 2, 1 (1969).

(11) L. Pauling, "The Nature of the Chemical Bond," 3rd ed, Cornell University Press, Ithaca, N.Y., 1960, pp 110, 464.

(12) L. Raff and H. A. Pohl, $\underline{Adv}$. $\underline{Chem}$. $\underline{Ser}$., 50, 173 (1965).

(13) (a) B. J. McAloon and B. C. Webster, $\underline{Theor}$. $\underline{Chim}$. $\underline{Acta}$, 15, 385 (1969); (b) G. Howat and B. C. Webster, $\underline{Ber}$. $\underline{Bunsenges}$. $\underline{Phys}$. $\underline{Chem}$., 75, 626 (1971).

FIGURE CAPTIONS

Figure 1. Models used in INDO calculations on the structure of the hydrated electron: (a) monomer shown with the coordinate axis system which defines the directions of the oxygen p orbitals for all models in this Figure and in Figure 3; (b) -(f) represent various dimer models incorporating aligned oxygen p orbitals of the individual molecules.

Figure 2. Variation of ρ_H^T for H_2O^- with the HOH angle for various OH bond lengths. Bond lengths are given in nm.

Figure 3. (a) A dimer model for the hydrated electron incorporating hydrogen bonding; (b) dimer model found to give lowest value of ρ_H^T. This model is planar with an OH bond length of 0.12 nm, an HOH angle of 105°, an oxygen-oxygen distance of 0.31 nm, and a distance between central hydrogens of 0.072 nm.

Table I: Values of ρ_H^T for Model (e) Multimers[a]

OH bond length nm	HOH angle degrees	O-O distance nm	ρ_H^T				$\dfrac{\rho_H^T \text{ (tetramer)}}{\rho_H^T \text{ (monomer)}}$
			monomer	dimer	trimer	tetramer	
0.11	105	0.18	0.644	0.533	0.480	0.443	0.69
0.11	105	0.20	0.644	0.537	0.519	0.448	0.70
0.12	105	0.18	0.706	0.537	0.463	0.383	0.54

[a]These geometries yielded minimum values of ρ_H^T for the tetramer.

Table II: Comparison of Spin Density Distributions for Monomers and Model (e) Tetramers with the Same Molecular Geometry[a]

OH bond length nm	HOH angle degrees	O-O distance nm	Species		ρ_H^b	ρ_O^s	ρ_O^{px}	ρ_O^{py}	ρ_O^{pz}
0.11	105	-----	monomer[c]		0.322	0.107	0.377	0.000	-0.128
0.11	105	0.18	tetramer[d]	(1.4)	0.015	0.015	0.055	-0.003	-0.005
				(2.3)	0.096	0.055	0.203	-0.008	-0.033
				total	0.222	0.140	0.516	-0.022	-0.076
0.11	105	0.18	tetramer[d]	(1,4)	0.012	0.010	0.050	-0.001	-0.004
				(2,3)	0.101	0.052	0.207	-0.003	-0.036
				total	0.226	0.124	0.514	-0.008	-0.080
0.12	105	-----	monomer[c]		0.352	0.085	0.397	0.000	-0.183
0.12	105	0.20	tetramer[d]	(1,4)	0.003	0.007	0.064	-0.001	-0.001
				(2,3)	0.093	0.040	0.246	-0.004	-0.044
				total	0.192	0.094	0.620	-0.010	-0.090

[a]These geometries yielded minimum values of ρ_H^T for the tetramers. [b]Refers to only one hydrogen nucleus. In all molecules the hydrogens are equivalent. [c]The monomer is considered to be in the xz plane as are the individual molecules of the tetramer (see Figure 1). [d]The molecules in the tetramer are equivalent in pairs.

Table III: Comparison of Spin Density Distributions for Monomer and Dimer Species Yielding Minimum ρ_H^T Values

Species[a]	O-O distance nm	H-H distance nm	ρ_H outer	ρ_H inner	ρ_O^s	$\rho_O^{P_x}$	$\rho_O^{P_y}$	$\rho_O^{P_z}$	ρ_H^T
monomer	----	----	0.352	0.352	0.085	0.397	-0.185	0.000	0.704
dimer (as in Fig. 3(b))	0.31	0.072	0.012 / 0.013	0.105 / 0.079	0.045 / 0.040	0.021 / 0.071	0.360 / 0.256	0.000 / 0.000	0.208
symmetrical dimer[b,c]	0.31	0.079	0.012	0.092	0.043	0.043	0.310	0.000	0.208
linear dimer[b,d]	0.33	0.090	0.018	0.091	0.041	0.064	0.287	0.000	0.217

[a]The molecular geometry is the same for all these species (OH bond distance = 0.12 nm, HOH angle = 105°).
[b]The molecules are equivalent. The total spin density associated with any type of orbital is thus twice the quoted value. [c]Planar configuration as in Fig. 3(b) except that the molecules have both been rotated until the center hydrogens are symmetrically placed with respect to the oxygen-oxygen axis. [d]Planar configuration as in Fig. 3(b) except that molecule 2 has been rotated until both inner hydrogens are linear with the oxygens.

17
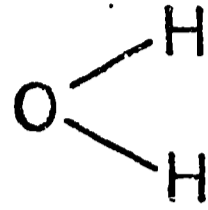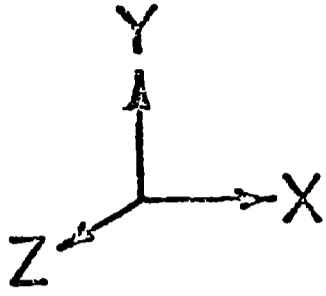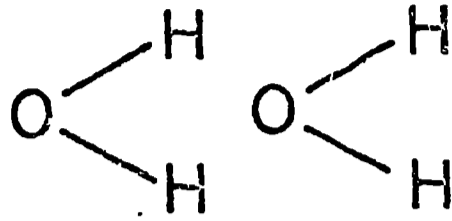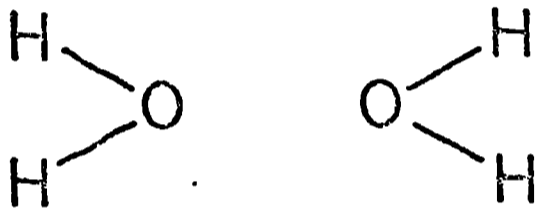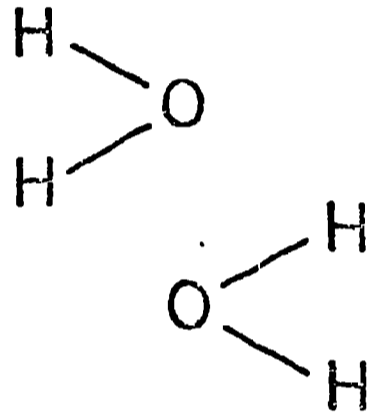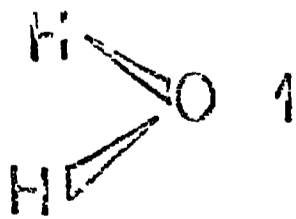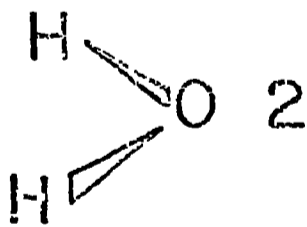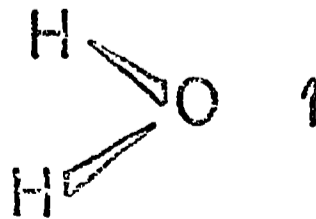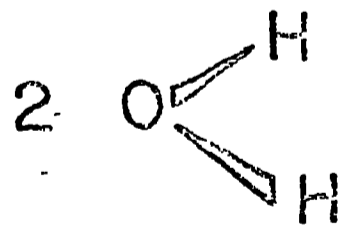
Figure 1   Kerr and Williams
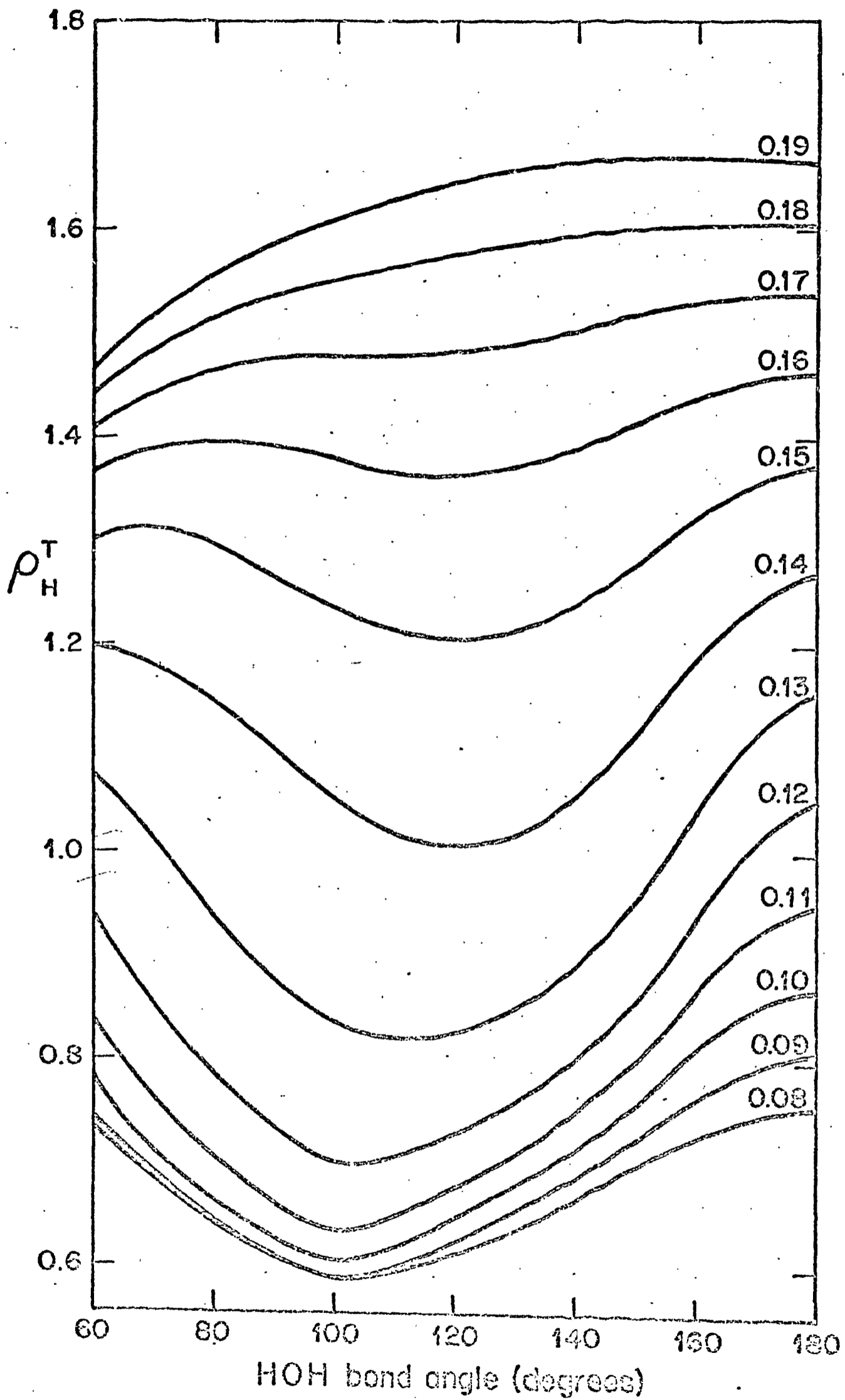
Figure 2   Kerr and Williams
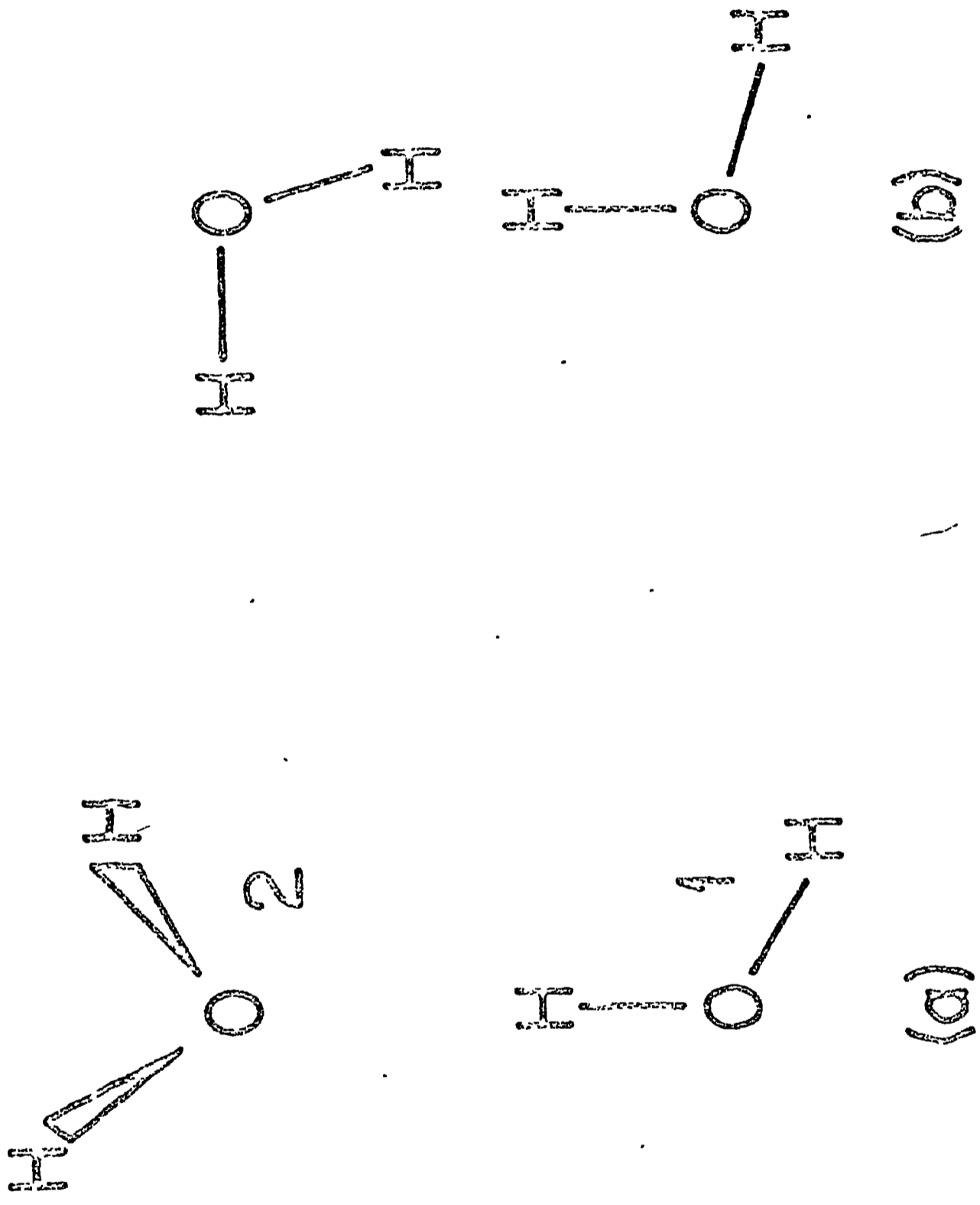
Figure 3   Kerr and Williams

Hydrogen Atom Abstraction by Methyl Radicals in Methanol Glasses at 67-77°K[1]

Alan Campion[2] and Ffrancon Williams[*]

Contribution from the Department of Chemistry, University of Tennessee, Knoxville, Tennessee 37916

Received

Abstract: It has been shown by esr studies that the thermal decay of $CH_3\cdot$ radicals in a methanol-$\underline{d}$ glass at 77°K proceeds with the concomitant formation of the $\cdot CH_2OD$ radical. The reaction obeys first-order kinetics over 75 percent of its course and there is reasonably good agreement between the rate constants as determined from $CH_3\cdot$ decay and $\cdot CH_2OD$ growth. At 77°K, the rates of H-atom abstraction by $CH_3\cdot$ from CH_3OD and CH_3OH are comparable but the rate of $CH_3\cdot$ decay in CD_3OD is slower by at least a thousandfold. This primary deuterium isotope effect confirms that abstraction occurs almost exclusively from the hydrogens of the methyl group. The apparent activation energy of 0.9 kcal mol^{-1} for the abstraction reaction in the glassy state at 67-77°K is much lower than the value of 8.2±0.2 kcal mol^{-1} previously reported for essentially the same reaction in the gas phase above 376°K. These findings are remarkably similar to those reported for H-atom abstraction by $CH_3\cdot$ radicals from acetonitrile and methyl isocyanide, and are consistent with the proposal that these reactions proceed mainly by quantum-mechanical tunneling at low temperatures. When $CH_3\cdot$ radicals are produced by the

1

photolysis of CH_3I and /of TMPD (N,N,N´,N´-tetramethyl-p-phenylenediamine)-CH_3Cl
with uv light in methanol, the contribution of hot radical processes to the
abstraction reaction appears to be negligibly small in comparison with the
rate of the thermal reaction.

Recent work in this laboratory has provided definitive evidence
for hydrogen atom abstraction by thermal methyl radicals in crystalline
acetonitrile[3] and methyl isocyanide[4] at 77°K and higher temperatures.
These reactions in the solid state are characterized by apparent activa-
tion energies (ca. 1.4 kcal mol^{-1} at 77°K[3]) which are much lower than the
value of 10.0 kcal mol^{-1} obtained for the corresponding reaction of methyl
radicals with acetonitrile above 373°K in the gas phase.[5] However, it has
been shown that these unusually low activation energies are consistent
with a very large contribution from quantum mechanical tunneling at low
temperatures.[6]

In contrast to the above findings, the importance of hydrogen atom
abstraction as a process responsible for the decay of alkyl radicals in
glassy matrices at low temperatures has not been clearly established.
Although abstraction reactions have been postulated in some systems,[7,8]
no evidence for product radical formation has been obtained despite
extensive kinetic studies[9] of alkyl radical decay in organic glasses,
and this latter work[9] has led to the conclusion that abstraction by thermal
radicals is unlikely to be significant at temperatures as low as 77°K.

To obtain unequivocal evidence for hydrogen atom abstraction, it is
necessary to establish a kinetic coincidence between the decay of the

reactant radicals and the formation of the product radicals. In principle, esr studies provide an ideal method for observing such a reaction, but there are serious practical difficulties when these studies are attempted in the solid state. Although the esr spectra of the reactant radicals are frequently well resolved in the case of simple alkyl radicals such as methyl and ethyl, the resulting product radicals would be expected to have broad ill-defined spectra in many of the glassy matrices usually employed. This basic difficulty has been overcome in the present investigation by using methanol-$\underline{d}$ as the glassy matrix since the esr spectrum of the $\cdot CH_2OD$ radical shows two fairly sharp lines which do not overlap significantly with the quartet spectrum of the $CH_3\cdot$ radicals.

Experimental Section

Materials and Preparation of Samples. Methanol (Fisher Certified A.C.S. grade) was dried $\underline{in\ vacuo}$ over powdered barium oxide, degassed, and distilled into breakseals for storage. Methanol-$\underline{d}$ (CH_3OD) was supplied by Diaprep Inc. and by E. Merck AG., Darmstadt. Methanol-$\underline{d}_4$ (CD_3OD) was obtained from Stohler Isotope Chemicals and E. Merck AG. Both of these deuterium-containing compounds were guaranteed by their manufacturers to be not less than 99% deuterated in the labeled positions. These materials were degassed and distilled into breakseals before use. Methyl chloride (The Matheson Co. Inc.) was used as received. Methyl iodide (Fisher Certified A.C.S. grade) was degassed, dried over magnesium sulfate, and

then distilled into breakseals which were stored in the dark. N,N,N,N'-
tetramethyl-p-phenylenediamine (TMPD) was received as the dihydrochloride
from Eastman Organic Chemicals (White Label grade). The free base was
released by adding excess alkali to an aqueous solution of the salt. The
solid TMPD was filtered and sublimed prior to use.

Samples of methanol, CH_3Cl, and TMPD were prepared as follows:
a methanolic solution of TMPD was syringed into an esr tube which was
then connected to the vacuum line with a ground glass joint. The methanol
was distilled off leaving   'r the TMPD in the esr tube. Methyl chloride
was admitted into the vacu.   from a cylinder and the required amount
condensed in a graduated tube. The needed amount of the appropriate
isotopic methanol was then added by distillation from the breakseal storage
ampoule. This mixture was subsequently distilled into the esr tube
which was then sealed under vacuum. The standard concentrations used in
this work were 0.2 mole % TMPD and 2 mole % CH_3Cl. On quenching the
sample to 77°K, a transparent glass was readily formed. The methanol
samples containing 2 mole % CH_3I as the only solute were prepared in a
similar fashion.

Ultraviolet Irradiation. Irradiations were carried out in the cavity
of the esr spectrometer with light from a B-H6 high-pressure mercury arc
lamp. The lamp was mounted in an Oriel Optics Corp. C-60-53 Universal
Lamp Housing equipped with a 2 inch condenser lens (uv-grade fused silica)
and a spherical rear-mirror reflector. A water filter reduced the intensity

of the unwanted ir radiation and a Pyrex (Corning 0-53) glass filter
eliminated most of the light below 290 nm. A secondary lens (fused silica)
was used to focus the beam on the irradiation slots of the cavity. Exposure
times could be controlled and reproduced fairly accurately through the use
of a shutter.

Esr Measurements. The esr spectrometer (Varian Model V-4502)
and associated equipment have been described.[10] Measurements were made
with the samples in a liquid nitrogen dewar which had an unsilvered
tail section extending through the sensitive region of the cavity.
Temperatures lower than 77.3°K were obtained by bubbling dry helium
gas through the liquid nitrogen,[11] and a constant temperature of 67±1°K
could easily be maintained. During the experiments involving this
technique, the temperature was monitored continuously with a copper-
constantan thermocouple placed in the esr dewar next to the sample tube.
The thermocouple leads were connected to the Digitec Thermocouple
Thermometer (United Systems Corp. Model 564) which had been calibrated
at 77.3°K.

Standard esr tubes of 2 or 3 mm i.d. made out of Spectrosil or
Suprasil quartz were employed, the smaller size being especially convenient
for use in the 67°K experiments. For long term experiments entailing
storage at 77°K for several days, it was necessary to use a different
design of sample tube[12] which could accommodate an internal standard so
that relative measurements were independent of day-to-day fluctuations

in instrument sensitivity. The tubes designed[12] for this purpose were

constructed from ca. 2 mm and 5 mm o.d. Suprasil tubing. The capillary

was inserted into the larger tube and sealed to it at both ends. This

provides an annular space to contain the sample material while the standard

may be placed inside the capillary. Ultramarine (Reckitts Blue) in chalk

was used as the standard in this work because its resonance occurs at

much lower field than that of the methyl radical and there is negligible

overlap between the spectra of sample and standard.

Results

Two methods[13] were employed to generate methyl radicals in the

various methanol glasses: the first depends on the photoionization of

TMPD and subsequent dissociative electron capture by methyl chloride,

and the second involves the photodissociation of methyl iodide. Both

of these techniques allowed the rapid _in situ_ generation of CH_3· radicals

within the spectrometer cavity, an important requirement in view of the

fast decay at the temperatures of interest. Although CH_3· radicals

are also formed efficiently by γ-irradiation of glasses containing methyl

halides,[9] this method was found to be much less useful for the present

purpose due to the significant decay which occurred during γ-irradiation

and transfer, even when the sample temperature was reduced to 67°K.

Most of the kinetic work to be described here was carried out with CH_3OD

rather than CH_3OH because the prominent low-field and center lines in

the triplet spectrum of ·CH_2OD are considerably sharper than the corres-

ponding lines from $\cdot CH_2OH$[14] which are broadened by hyperfine interaction with the hydroxyl proton.

Recordings of esr spectra taken from a typical kinetic experiment are presented in Figure 1. Comparison of Spectrum A with Spectrum B shows that the decay of the $CH_3\cdot$ quartet signal is accompanied by the appearance of new spectral features. These are more clearly revealed as the sharp lines in the residual Spectrum C which can be definitely assigned to $\cdot CH_2OD$.[14] Since these lines are not present in Spectrum A, it can be inferred that the spectrum of $\cdot CH_2OD$ grows in during the decay of the $CH_3\cdot$ quartet. However, this conclusion rests on the assumption that the prominent lines of the $\cdot CH_2OD$ spectrum are not obscured by the more intense lines of the $CH_3\cdot$ quartet in the original spectrum. To verify this point, an experiment was carried out in which the sample was re-irradiated briefly after the lines from $\cdot CH_2OD$ became clearly recognizable in the spectra recorded after the first photolysis. The results in Figure 2 show that the sudden large increase in the intensity of the $CH_3\cdot$ quartet has very little effect on the signal heights of the two sharp lines assigned to $\cdot CH_2OD$ and, as expected, the subsequent decay of $CH_3\cdot$ leads to a further growth of $\cdot CH_2OD$. Thus, it can be confidently asserted that the appearance of $\cdot CH_2OD$ during the thermal decay of $CH_3\cdot$ is real and not an experimental artifact.

The thermal reaction was followed by repetitive scanning at 1 min intervals. Kinetic measurements were made using lines 1 and 3 (from low

field) of the $CH_3\cdot$ quartet and the two sharp components of the $\cdot CH_2OD$

spectrum. For the analysis of several kinetic runs, a computer program was

used to subtract out the contribution of the $CH_3\cdot$ radical spectrum from

the composite spectrum. The original $CH_3\cdot$ spectrum was employed for this

purpose after normalization to the observed intensity. This procedure

did not yield signal heights for $\cdot CH_2OD$ significantly different from those

obtained by direct measurement, providing further confirmation that there

is negligible overlap between the pertinent components in the spectra

of these two species. Accordingly, the actual signal heights were taken

as proportional to the radical concentrations. It would have been valuable

to obtain the stoichiometric relationship between $CH_3\cdot$ decay and $\cdot CH_2OD$

growth but accurate estimates were precluded by the overall anisotropy

of the $\cdot CH_2OD$ spectrum.

The decay of $CH_3\cdot$ radicals in CH_3OD is described fairly well by

first-order kinetics over the first 75 percent of the reaction. Actually,

for a typical set of data derived from a single kinetic run, the fit to

standard first-order and second-order plots was about equally good. However,

the first-order rate constant was found to be independent of the initial

$CH_3\cdot$ radical concentration when this was varied by a factor of four, and

this criterion led to the adoption of first-order kinetics for the reaction.

In the later stages of $CH_3\cdot$ decay, the concentration declined at a slower

rate than that represented by an extension of the first order plot. Previous

workers[15,16] have also observed deviations from linear first-order plots

for the decay of alkyl radicals in organic glasses.

As indicated by the parallel plots in Figure 3 and by the comparison of data in Table I, there is satisfactory agreement between the rate constants calculated independently from $CH_3\cdot$ decay and $\cdot CH_2OD$ formation. For the system (TMPD-CH_3Cl-CH_3OD) which has been studied most thoroughly, the agreement is particularly good and well within the reproducibility (±20 percent) of these data. This demonstration of kinetic coincidence clearly establishes the abstraction reaction in the CH_3OD glass.

Reference to Table I shows that similar kinetic results were obtained when the methyl radicals were generated by the photolysis of CH_3I in CH_3OD. Incidentally, it was noticed that the increase in the $\cdot CH_2OD$ signal height relative to the initial $CH_3\cdot$ signal was less after CH_3I photolysis than after TMPD-CH_3Cl photolysis, suggesting that the $\cdot CH_2OD$ components are selectively broadened in the CH_3I system.

The temperature dependence of the abstraction rate constant (Table I) corresponds to an apparent activation energy of $\underline{ca}$. 0.9 kcal mol^{-1} between 67 and 77°K. In view of this very small temperature coefficient, it should be possible to extend the kinetic measurements to even lower temperatures in future work with additional cryogenic facilities.

Additional studies with CH_3OH and CD_3OD glasses provide evidence for a specific deuterium isotope effect. Although the measurements in CH_3OH are subject to a greater uncertainty because the $\cdot CH_2OH$ spectral components are not as well resolved, the rate constants for the abstraction reactions in the CH_3OH and CH_3OD glasses (Table I) are comparable.

In contrast, the decay of $CH_3 \cdot$ in CD_3OD was found to be slower than in CH_3OH or CH_3OD by more than three orders of magnitude under corresponding conditions. This large deuterium isotope effect is consistent with the previous demonstration that abstraction occurs from the hydrogens of the methyl group.

In view of the many observations in the literature regarding the prevalence of hot radical reactions in photolytic processes,[17] an investigation of this possibility in the present systems seemed to be desirable. Since a hot radical reaction would be expected to show little selectivity between H and D atom abstraction, the photolysis (with Pyrex filter) of $TMPD-CH_3Cl$ and of CH_3I was studied in CD_3OD. In each case, photolysis for 10 min (as compared to 5 sec employed in the CH_3OH and CH_3OD studies) produced a high concentration of $CH_3 \cdot$ radicals but failed to result in the growth of a signal attributable to either $\cdot CD_2OD$ or $D\dot{C}O$, the latter being a possible photolysis product of $\cdot CD_2OD$. Even when the photolysis of CH_3I was carried out with unfiltered uv-light having considerable intensity at 2500 Å, only $CH_3 \cdot$ and a much smaller yield of $CD_3 \cdot$ radicals (the latter were produced by the photolysis of the CD_3OD matrix) were observed and there was no significant production of radicals resulting from deuterium atom abstraction.

In an effort to observe deuterium atom abstraction by thermal $CH_3 \cdot$ radicals from CD_3OD at higher temperatures than those used in the preceding studies with CH_3OH and CH_3OD, the CD_3OD matrix was warmed to ca. 108°K

at which point the $CH_3 \cdot$ radicals decayed out very rapidly without the observation of any product radical.

Discussion

This work provides what appears to be the first convincing demonstration of a thermal H-atom abstraction reaction in a glass at low temperature. The primary evidence consists of the unambiguous identification of the product radical together with the good agreement between the rate constants as determined from $CH_3 \cdot$ decay and $\cdot CH_2OD$ (or $\cdot CH_2OH$) growth. Supporting evidence is provided by a comparison of the decay rates in CH_3OH, CH_3OD, and CD_3OD which establishes that abstraction occurs almost exclusively from the methyl hydrogens and shows the expected large primary deuterium isotope effect.

In the absence of information about the stoichiometry of the reaction, the kinetic results obtained here do not exclude other paths of $CH_3 \cdot$ decay in parallel with abstraction. The possibility of a competition between abstraction and recombination processes should therefore be considered, especially since a similar reaction scheme has been definitely established in the crystalline acetonitrile systems.[3,12,18] For the TMPD-CH_3Cl systems investigated here, the recombination reactions could in principle involve both a reaction between two $CH_3 \cdot$ radicals as well as geminate recombination of the $CH_3 \cdot$ radical with the chloride ion. Indeed, the latter reaction has been postulated[9,16] to account for the decay of $CH_3 \cdot$ radicals which

were similarly generated in hydrocarbon and 2-methyltetrahydrofuran glasses, but no supporting esr evidence was obtained.[13,15,16]

If a significant fraction of the $CH_3 \cdot$ decay in CH_3OH and CH_3OD were to occur by combination of two separated $CH_3 \cdot$ radicals, diffusion would be involved. However, the extremely slow decay of $CH_3 \cdot$ radicals in CD_3OD as compared to that in CH_3OH and CH_3OD would then correspond to a solvent isotope effect of more than 10^3. This is entirely unreasonable considering that no isotope effect is observed for CH_3OD, and consequently it is thought that the combination reaction is unlikely to contribute to $CH_3 \cdot$ decay in this system. Turning to the possibility of the geminate recombination process, no evidence was obtained in the present work for a recombination product, although esr spectra attributable to weakly interacting methyl radical-halide ion pairs have been observed in a crystalline matrix.[19]

The apparent activation energy of ca. 0.9 kcal mol^{-1} for the H-atom abstraction reaction by $CH_3 \cdot$ from CH_3OD in solid methanol at 67-77°K is very much lower than the value of 8.2 ± 0.2 kcal mol^{-1} reported for essentially the same reaction ($CH_3 \cdot$ with CH_3OH) at 376-492°K in the gas phase.[20] Calculation of the Arrhenius pre-exponential factor from the low temperature data gives a value of 1.1 sec^{-1} which is much lower than the vibration frequency of ca. 9×10^{13} sec^{-1} assumed in some recent calculations[6] for a non-tunneling reaction. The general similarity of these results to those for the corresponding abstraction reaction from acetonitrile is striking and suggests a common explanation for the anomolously low activation energy and pre-exponential factor in the low temperature region. Quantum mechanical

tunneling has been proposed to account for this behavior,[6] and the present results lend further credence to this hypothesis. On the other hand, if the correct explanation for the low activation energies were to reside in "cage effects" by which the potential energy surfaces become modified for reactions in the solid state, it might be expected that such effects would be very sensitive to the difference between crystalline and glassy solids. From the results for acetonitrile and methanol considered here, this does not appear to be the case. However, a more definitive test of the importance of "cage effects" would result from a comparison of results for the same reaction in a crystalline and glassy matrix. Further work is planned on the methanol system with this idea in mind.

This work demonstrates that hydrogen atom abstraction can occur by a thermal reaction at low temperatures on a timescale which is short compared to the irradiation times commonly employed in many photochemical and radiation chemical experiments with solid matrices. Hence, under these conditions, caution should be exercised in attributing all the trapped intermediates present after photolysis or radiolysis at low temperatures to the results of primary processes and hot radical reactions. Also, since the present results in CD_3OD provide no evidence for abstraction by hot radical reactions in the photolysis of CH_3I and $TMPD-CH_3Cl$ in methanol, it would seem that the importance of such processes[9,17] may be critically dependent on the nature of the matrix.

REFERENCES

(1) This research was supported by the U.S. Atomic Energy Commission under Contract No. AT-(40-1)-2968, and this is AEC Document No. ORO-2968-74.

(2) Undergraduate on leave from New College, Sarasota, Fl. 33578.

(3) E. D. Sprague and F. Williams, J. Amer. Chem. Soc., 93, 787 (1971).

(4) J.-T. Wang and F. Williams, ibid., in press.

(5) M. H. J. Wijnen, J. Chem. Phys., 22, 1074 (1954).

(6) R. J. Le Roy, E. D. Sprague, and F. Williams, J. Phys. Chem., 76, 546 (1972).

(7) H. S. Judeikis and S. Siegel, J. Chem. Phys., 43, 3625 (1965).

(8) C. U. Morgan, J. Amer. Chem. Soc., 91, 1599 (1969).

(9) J. E. Willard in "Fundamental Processes in Radiation Chemistry," P. Ausloos, Ed., Interscience-Wiley, New York, N.Y., 1968, p 599.

(10) J. Lin, K. Tsuji, and F. Williams, J. Amer. Chem. Soc., 90, 2766 (1968).

(11) F. W. Lytle and J. T. Stoner, Science, 148, 1721 (1965).

(12) E. D. Sprague, Ph.D. Dissertation, The University of Tennessee, 1971.

(13) R. F. C. Claridge and J. E. Willard, J. Amer. Chem. Soc., 87, 4992 (1965).

(14) P. J. Sullivan and W. S. Koski, ibid., 85, 384 (1965).

(15) M. Shirom and J. E. Willard, J. Phys. Chem., 72, 1702 (1968).

(16) W. G. French and J. E. Willard, ibid., 72, 4604 (1968).

(17) C. D. Bass and G. C. Pimentel, J. Amer. Chem. Soc., 83, 3754 (1961).

(18) K. Takeda and F. Williams, J. Phys. Chem., 74, 4007 (1970).

(19) E. D. Sprague and F. Williams, J. Chem. Phys., 54, 5425 (1971).

(20) A. F. Trotman-Dickenson and E. W. R. Steacie, ibid., 19, 329 (1951).

Table I. Experimental Rate Constants for Hydrogen Atom Abstraction by Methyl Radicals from Methanol-h and Methanol-d in the Glassy State

Temperature °K	Source of $CH_3\cdot$ Radicals	Glass	No. of Runs	Rate Constant[a]	
				k^{b}	k^{c}
				min^{-1}	
77	TMPD-CH$_3$Cl	CH$_3$OH	2	0.14	0.20
77	TMPD-CH$_3$Cl	CH$_3$OD	9[d]	0.19(0.20)[e]	0.21(0.23)[f]
77	CH$_3$I	CH$_3$OD	2	0.20	0.30
67	TMPD-CH$_3$Cl	CH$_3$OD	4	0.07	0.10

[a]Based on first-order plot of measurements over the first 75 percent of reaction. [b]From decay of line 3 of CH$_3\cdot$ quartet. [c]From growth of $\cdot$CH$_2$OD or $\cdot$CH$_2$OH center line. [d]The standard deviation for the rate constants obtained in this group of runs is 20 percent of the mean value. [e]Value in parentheses determined from decay of line 1 of CH$_3\cdot$ quartet. [f]Value in parentheses determined from growth of low-field line from $\cdot$CH$_2$OD.

CAPTIONS TO FIGURES

Figure 1. Esr spectra of TMPD-CH_3Cl-CH_3OD system at 77°K recorded immediately after 5 sec photolysis (A), after 6 min (B), and after 90 min (C). Spectrum C was recorded at a gain of 2.5 times that used to record the other two spectra.

Figure 2. Esr spectra of TMPD-CH_3Cl-CH_3OD system at 77°K recorded under the same conditions (A) 9 min after an initial photolysis for 5 sec, (B) 1 min later and immediately after a second photolysis for 10 sec, and (C) 3 min after the second photolysis.

Figure 3. First-order kinetic plots derived from measurements on esr spectra after photolysis of TMPD-CH_3Cl-CH_3OD at 77°K: (O), CH_3 decay; ( ), CH_2OD growth; the corresponding λ_t values represent the signal heights for the low-field outer line of the $CH_3 \cdot$ quartet and the center line of the $\cdot CH_2OD$ spectrum recorded at the same gain.
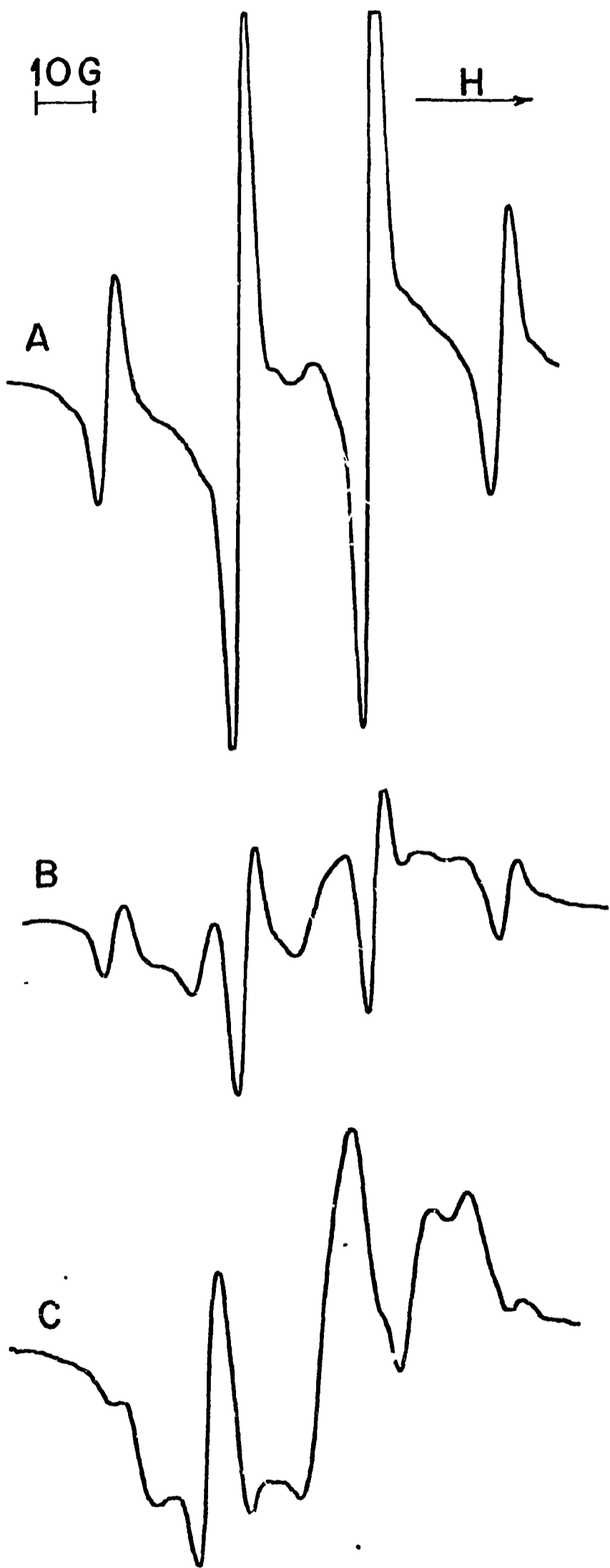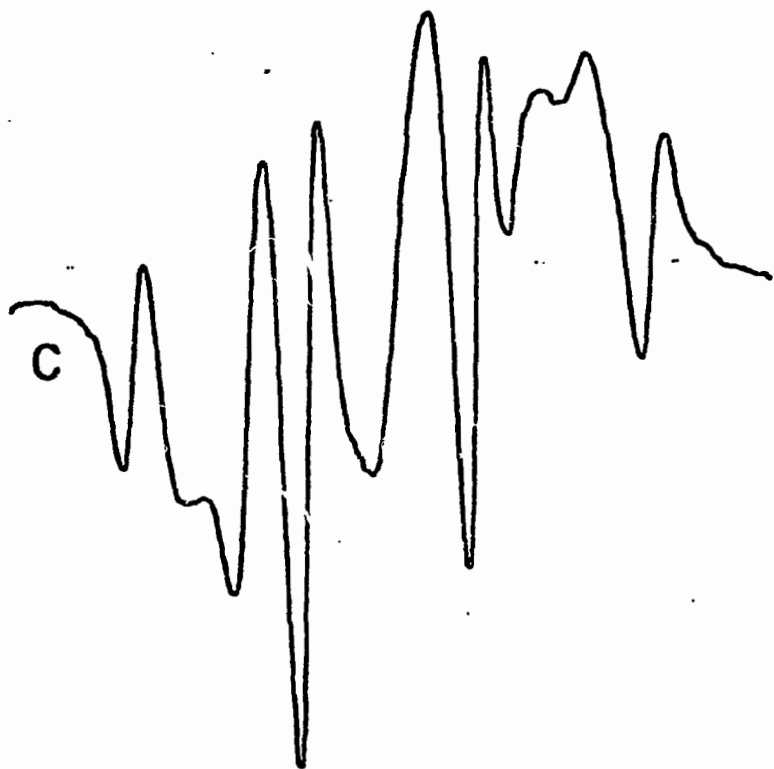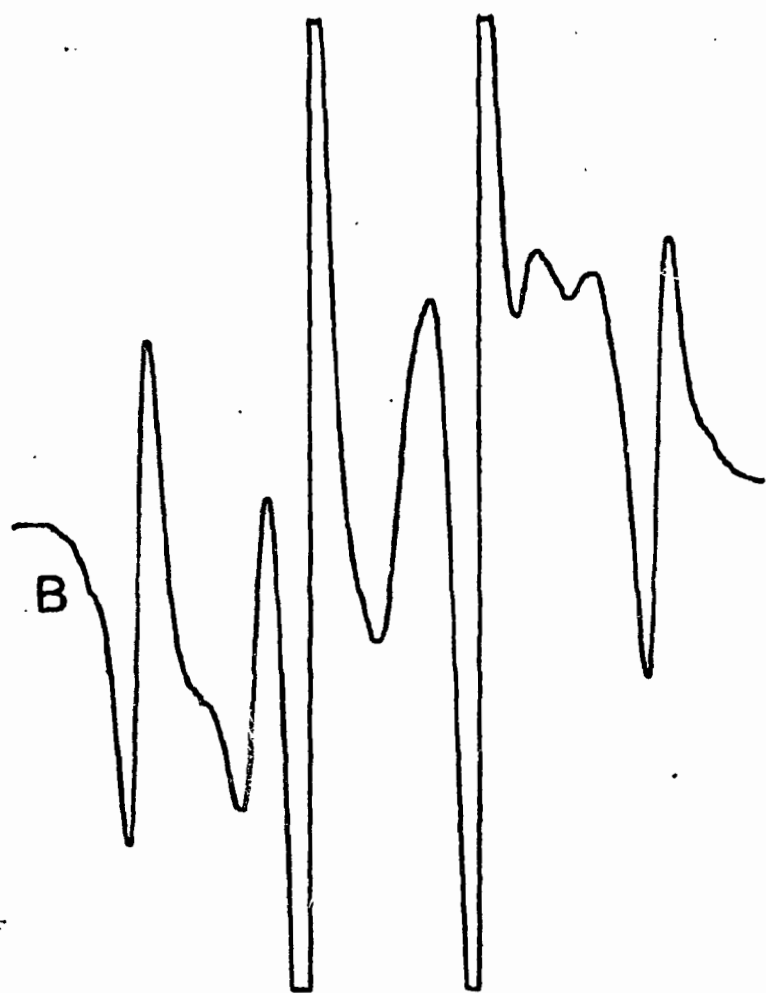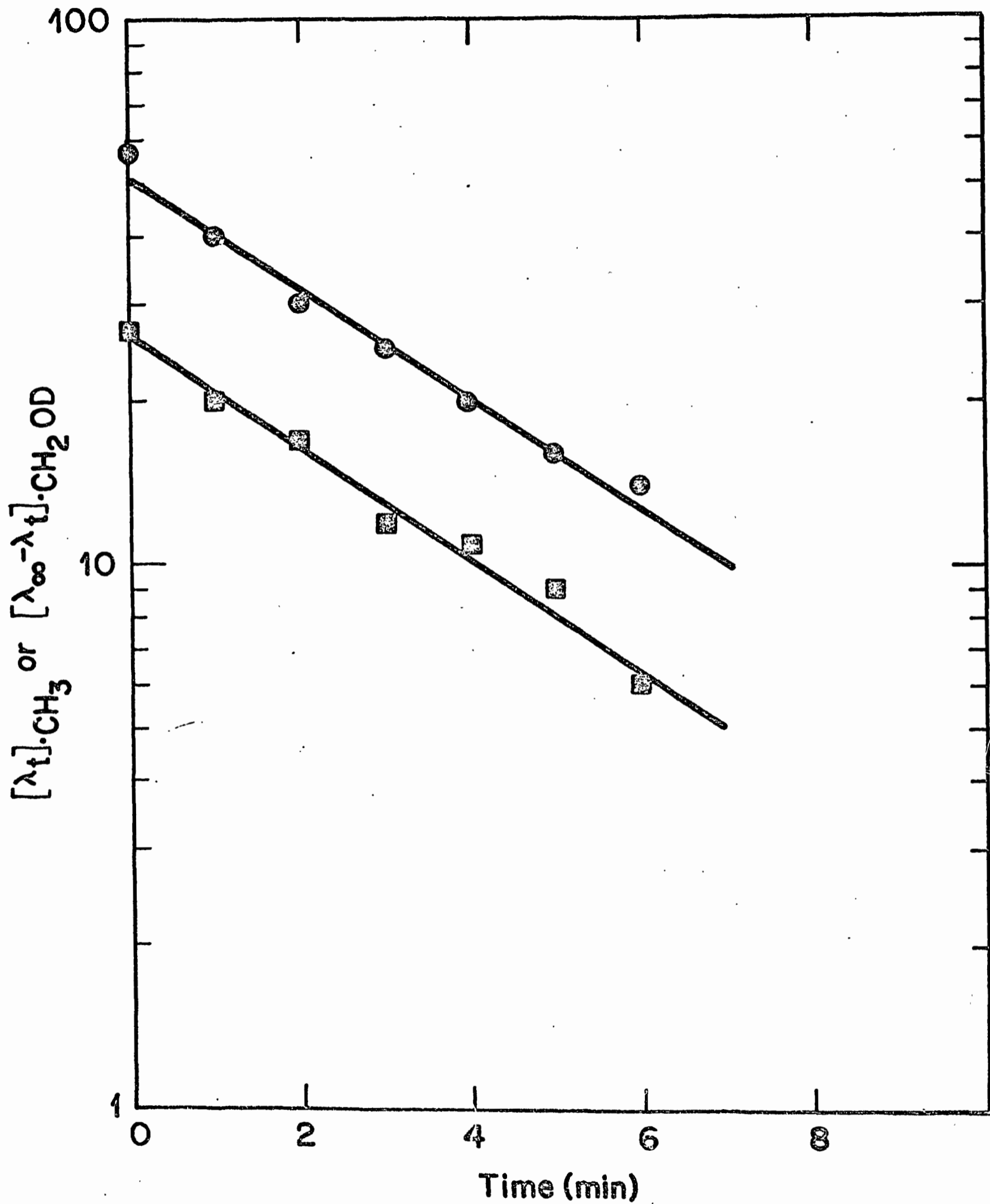
10 G

H →

A

B

C

ESR STUDIES OF ALIPHATIC RADICAL ANIONS

AND RADICAL-ANION PAIRS

IN γ-IRRADIATED CRYSTALLINE SOLIDS

M. A. Bonin, Y. J. Chung, E. D. Sprague,[*] K. Takeda,[†]

J. T. Wang, and F. Williams

Department of Chemistry, University of Tennessee,

Knoxville, Tennessee   37916,   USA

INTRODUCTION

It is well known that many organic molecules possessing low-lying orbitals form radical anions by electron attachment, and that several of these radical anions can initiate vinyl polymerization. However, there have been relatively few ESR studies of simple aliphatic radical anions, presumably because these species are generally too unstable to be observed under conventional experimental conditions in the liquid state. To some extent, this limitation set by the intrinsic chemical stability can be overcome by solid state studies at low temperatures, and this paper summarizes recent ESR work in this laboratory dealing with the identification and reactions of aliphatic

[*] Present address: Max-Planck-Institut für Kohlenforschung, Mülheim, West Germany

[†] Present address: Fuji Photo Film Co. Ltd., Research Laboratories, Tokyo, Saitama, Japan   351

radical anions in γ-irradiated crystalline solids. Incidental

to this research, evidence has been obtained for weakly interacting

radical-anion pairs formed by the dissociation of certain radical

anions. Another aspect of this work which has received particular

attention but will not be discussed here concerns the unexpected

occurrence of hydrogen atom abstraction reactions by methyl radicals

at 77°K (Sprague & Williams, 1971a). Detailed kinetic studies on

a number of different systems (Wang & Williams, 1972) provide strong

evidence for a large contribution from quantum mechanical tunneling in

such reactions at low temperatures (LeRoy, Sprague & Williams, 1972).

RESULTS AND DISCUSSION

Only a brief survey of the main findings will be given here, and

many historical and experimental details are of necessity omitted.

Since the results are highly characteristic for each compound and even

for the particular crystalline state in which it is γ-irradiated, each

system is discussed separately.

Acetonitrile Crystal I

The photobleachable colour center produced by γ-irradiation of

the metastabilized high-temperature phase of acetonitrile at 77°K has

been identified as the dimer radical anion (Sprague, Takeda & Williams,

1971). All the ESR studies on the structure of the radical anions of

acetonitrile have been carried out with deuterated compounds since the corresponding ESR spectra in CH_3CN are virtually unobservable because of proton hyperfine broadening and overlapping signals from other radicals. Representative ESR spectra from aligned crystals of $CD_3C^{14}N$ and $CD_3{}^{13}C^{14}N$ are presented in Figure 1 and show hyperfine interaction of the unpaired electron with pairs of magnetically equivalent nuclei derived from two acetonitrile molecules. These results together with those for $CD_3C^{15}N$ and $^{13}CD_3C^{14}N$ establish that the dimer radical anion possesses a center of symmetry, as provided by an antiparallel placement of molecules.

The experimental spin densities derived from the principal values of the hyperfine tensors (Takeda, 1971) show that the unpaired electron resides mainly in a single 2p orbital on each nitrogen atom ($\Sigma\rho_N = 0.68$) and the remaining fraction is accounted for by the spin densities on the methyl carbon ($\Sigma\rho_C^{CD_3} = 0.13$) and on the cyanide carbon ($\Sigma\rho_C^{CN} = 0.27$). Recent INDO calculations (Kerr, unpublished work) based on the structure shown in Figure 1 are in good agreement with these results and confirm the previous assignment (Sprague, Takeda & Williams, 1971) of the nitrogen spin density to the in-plane 2p orbitals between the molecules.

Evidence which establishes the anionic nature of the species comes from the results of photobleaching and electron scavenging experiments. The purple colour and the ESR spectrum of the dimer species in CD_3CN are removed on bleaching with red or white light

(Bonin, Tsuji & Williams, 1968), and the only product observable
by ESR is the $CD_3 \cdot$ radical. Additional experiments with CH_3CN and
$^{13}CD_3CN$ have verified that photodisociation gives the corresponding
methyl radicals, so that the overall process can be represented by
the equation,

$$(CD_3CN)_2^{\overline{\cdot}} \xrightarrow{h\nu} CD_3 \cdot + CN^- + CD_3CN$$
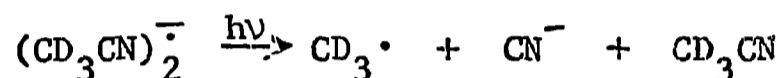
It is remarkable that this photobleaching reaction is thermally
reversible, and the dimer radical anion recovers completely in CD_3CN.
The reaction occurs slowly on standing at 87°K ($t_{1/2} \sim 12$ min) but
takes place within a few minutes at 100°K ($t_{1/2} \sim 1$ min). On the
other hand, the recovery of the dimer radical anion in CH_3CN is much
less complete, particularly below 100°K, and some of the methyl radicals
decay irreversibly. This difference between the reactions in CD_3CN and
CH_3CN is due to the intervention of a competitive process of hydrogen
atom abstraction by the methyl radical from a neighboring CH_3CN molecule
(Takeda & Williams, 1970), a reaction which exhibits a very large
primary deuterium isotope effect (Sprague & Williams, 1971). The
kinetics of these reactions have been studied extensively (Bonin, 1969;
Sprague, 1971; Wang, 1972).

Definite confirmation that the dimer species is an anion rather
than a cation is supplied by the results obtained using CD_3CN doped with
methyl halides as competitive electron scavengers (Sprague & Williams,
1971b). In mixtures containing 10 mole % of CH_3Cl or CH_3Br, dimer radical

anion formation is presented and scavenging is complete as evidenced
by the absence of colour and the lack of any photobleaching effect on
the ESR spectrum of the sample after γ-irradiation. Unexpectedly,
the product of the scavenging reaction is of intrinsic interest. For
the CH_3Br/CD_3CN mixture, the upper spectrum presented in Figure 2A can
be analyzed into two separate quartets of quartets as indicated by the
stick diagram, and these can be assigned to $CH_3\cdot$ radicals interacting
with bromide ions ($^{79}Br^-$ and $^{81}Br^-$ are present in almost equal abundance).
When the sample was pulse annealed, the spectrum changed to that of the
familiar quartet due to free $CH_3\cdot$ radicals (see Figure 2A) showing that
dissociation of the methyl radical-bromide ion pairs had occurred. As
well as furnishing evidence that the paramagnetic dimer species in CD_3CN
results from electron attachment, this experiment provides spectroscopic
proof of dissociative electron capture by CH_3Br. Since the proton
splitting in the spectrum of the unannealed sample is about 90% of the
value for the free $CH_3\cdot$ radical, it seems more appropriate to describe
the original species as a methyl radical-bromide ion pair than a methyl
bromide radical anion.

The incorporation of methyl isocyanide into acetonitrile crystal I
also resulted in efficient electron scavenging by the solute during
γ-irradiation, and at sufficiently high concentration of scavenger
(10 mole % CH_3NC in CD_3CN), the dimer radical anion of acetonitrile was
not produced. In this case $CH_3\cdot$ radicals were produced directly during
γ-irradiation so they must have originated from dissociative electron
capture by CH_3NC (Wang, 1972). Although the reaction products are

presumably identical to those (methyl radical and cyanide ion)
produced on photodissociation of the acetonitrile dimer radical
anion, no evidence was obtained for the generation of a photo-
bleachable radical anion in a subsequent thermal recombination
reaction. The loss of $CH_3 \cdot$ radicals by competitive hydrogen atom
abstraction from CH_3NC (Wang and Williams, 1972) should be relatively
unimportant in a largely deuterated matrix, so the failure to observe
recombination can probably be attributed to the inverted position of
the cyanide ion in the acetonitrile lattice.

Acetonitrile Crystal II. The lower crystalline phase of ace-
tonitrile is prepared by slow cooling of the sample through a phase
transition (Putnam, McEachern & Kilpatrick, 1965) at 215°K, about
12° below the melting point. On γ-irradiation of this phase at
77°K, the monomer radical anion is produced (Takeda & Williams,
1969). The identification is based largely on ESR studies of
γ-irradiated $CD_3C^{14}N$ and $CD_3{}^{13}C^{14}N$. Although it is extremely
difficult to grow single (aligned) crystals of this lower phase, this
was achieved in some instances and particularly well resolved spectra
were obtained in the case of $CD_3{}^{13}C^{14}N$.

A photobleachable triplet spectrum (Figure 1) is produced in
$CD_3C^{14}N$ indicating that the unpaired electron interacts with only one
^{14}N nucleus. This is verified by the single crystal spectrum from
$CD_3{}^{13}C^{14}N$ which is seen to consist of a doublet of triplets with a

large ^{13}C splitting. The principal values of the ^{13}C(CN) hyperfine tensor in gauss are [71.7, 59.6, 53.0] from which the spin densities in the 2s and in-plane 2p orbitals of the cyanide carbon are calculated to be 0.06 and 0.19, respectively. These values give a p/s hybridization ratio of 3.51 and by a well known formula (Atkins & Symons, 1967) this leads to a calculated CCN angle of 130°. This result corresponds closely to the HCN angle of 131° in the isostructural molecule HCN$^-$ (Adrian et al., 1969). The structure of the acetonitrile monomer radical is indicated in Figure 1 and it should be noted that the total spin density on the carbon in the cyanide group ($\rho_C^{CN} = 0.32$) is slightly larger than that on nitrogen ($\rho_N = 0.29$). This is expected in view of the electronegativity difference between carbon and nitrogen which should concentrate the charge distribution in the antibonding orbital more in favour of the carbon of the cyanide group. Another point of interest is the presence of substantial spin density on the carbon of the methyl group ($\rho_C^{CD3} = 0.31$). The large isotropic ^{13}C splitting of $\sim$ 88 gauss from this carbon suggests that in the contributing structure $CD_3 \cdot CN^-$, the configuration at the methyl carbon atom is tetrahedral rather than planar.

The photobleaching and thermal recovery reactions of the acetonitrile monomer radical anion are strikingly similar to those already described for the dimer species in Crystal I, thereby providing strong confirmation of the radical anion assignment. Recovery of the

monomer radical anion from the methyl radical produced on photo-dissociation proceeds to completion in CD_3CN as before, but the reaction rate for monomer recovery in Crystal II is about a factor of ten slower than that for dimer recovery in Crystal I at the same temperature although the activation energies have very nearly the same value (4.5 ± 0.5 kcal mole^{-1}) within experimental error. In the case of CH_3CN the recovery reaction competes with hydrogen atom abstraction by methyl radicals, again paralleling the results in Crystal I.

Adiponitrile. Monomer and dimer radical anions of $NC(CD_2)_4CN$ have also been identified by ESR. The monomer radical anion is formed by γ-irradiation at 77°K of the crystalline phase produced directly from the melt whereas the dimer is produced on irradiation of the phase prepared by crystallization from the glass at low temperature. Excellent single crystals of the former phase were grown and enabled the determination of the principal values for the ^{14}N hyperfine tensor of the monomer radical anion (Takeda, 1971). These values in gauss are [21,0,0] which hardly differ from the corresponding results for HCN^- (Adrian et al., 1969). Only powder spectra could be obtained from the other crystalline phase but the parallel features of a quintet ESR spectrum are clearly displayed with $A_{||}$ (^{14}N) = 17.2 gauss which is almost identical to that found for the dimer radical anion in acetonitrile Crystal I. Both monomer and dimer radical anions are photobleached but only the monomer shows appreciable thermal recovery.

Succinonitrile. In contrast to the results for acetonitrile

and adiponitrile, the dimer radical anion is formed in both crystalline

phases of succinonitrile. Identification is based in each case on the

powder ESR spectrum of succinonitrile-d_4 which closely resembles the

corresponding spectra of the dimer radical anions of acetonitrile,

propionitrile, and adiponitrile. The formation of the $\cdot CH_2CH_2CN$

radical is observed in both crystal phases of succinonitrile-h_4 after

photobleaching but it is remarkable that thermal recovery to the dimer

radical anion proceeds only in Crystal II (Campion & Williams, 1971).

Similar results were obtained with succinonitrile-d_4. Presumably the

radical produced on photobleaching in Crystal I relaxes to a position

in the lattice which prevents the regeneration of the dimer radical

anion.

Acrylonitrile. The ESR spectra of γ-irradiated acrylonitrile

differ according to the nature of the crystalline phase (Chung, Takeda

& Williams, 1970). A photobleachable triplet spectrum was observed

in the low-temperature phase and has been tentatively assigned to the

monomer radical anion. Only the spectrum of the $CH_3 \overset{\cdot}{C}HCN$ radical could

be identified in quenched samples of the high-temperature phase.

tert-Butyl Isocyanate. The ESR spectrum of crystalline tert-

butyl isocyanate after γ-irradiation (Figure 3A) shows the well resolved

lines of the tert-butyl radical spectrum with a hfs of 22.0 gauss and

three central components with a hfs of 4.8 gauss. The latter structure

is selectively removed by photobleaching with visible light and this change is accompanied by a considerable increase in the intensity of the tert-butyl radical spectrum, as shown in the lower spectrum of Figure 3A. By analogy to the studies on nitriles, the photobleachable species with the triplet spectrum can be assigned to the radical anion of tert-butyl isocyanate. Further evidence for this assignment comes from experiments using samples doped with tert-butyl iodide, an effective electron scavenger. As shown in Figure 2B, a rather complicated ESR spectrum is obtained after such mixtures are γ-irradiated at 77°K, and there is no photobleaching effect, suggesting that electron scavenging has occurred. On rapid annealing at higher temperatures, the spectrum gradually changes to that of the tert-butyl radical. Although the original spectrum of the doped sample is not easily analyzed, it can be interpreted reasonably well as the spectrum of tert-butyl radical-iodide ion pairs formed when tert-butyl iodide undergoes electron capture. The thermal dissociation of these radical-anion pairs parallels the results (Figure 2A) for the methyl radical-bromide ion pairs in acetonitrile Crystal I.

tert-Butyl Isothiocyanate. As shown in the upper spectrum of Figure 3B, the ESR spectrum of γ-irradiated tert-butyl isothiocyanate is composed of both a broad singlet feature and the multiplet spectrum of the tert-butyl radical. This particular spectrum was recorded while the sample was exposed to red light and the lines of the tert-butyl radical

multiplet are much sharper than in the spectrum recorded with the
sample in the dark, although the singlet feature was unaffected. This
effect of line sharpening by red light was found to be completely
reversible. On illuminating the sample with unfiltered tungsten light,
the singlet spectrum was photobleached irreversibly and there was
a large increase in the intensity of the tert-butyl radical spectrum,
as shown in the middle spectrum of Figure 3B recorded during this
exposure to visible light. When the lamp was turned off, the lines
of the tert-butyl radical spectrum broadened. Again these lines could
be sharpened by illumination with red light and the relative increase
in signal height was similar to that observed before photobleaching.
Further experiments showed that light in the near-infrared region
(λ > 1250 nm) was responsible for the photodynamic effect on the tert-
butyl radical spectrum in this system (Chung & Williams, 1972).

On the basis of the photobleaching reaction, the singlet spectrum
is assigned to the radical anion. Since the reversible line broadening
is observed for the tert-butyl radicals produced by photodissociation of
the radical anion as well as those formed directly by γ-irradiation,
this suggests that the broadening is due to the interaction of the tert-
butyl radical with the thiocyanate anion. Moreover, a strong resemblance
to the alkyl radical-halide ion pairs is indicated by comparison with
the spectrum of the methyl radical-chloride ion pair which consists of
the familiar quartet spectrum of the methyl radical broadened by hyperfine
coupling with the chloride ion (Sprague, 1971). Although the exact nature
of the magnetic resonance interaction responsible for line broadening in
the tert-butyl radical-thiocyanate anion pair is not directly evident,

the reversible photodynamic behavior can probably be attributed to motional effects which lead to an overall reduction in the $\underline{g}$ anisotropy (Chung & Williams, 1972).

SUMMARY

This paper has been concerned with the identification and reactions of radical anions and radical-anion pairs derived by electron attachment to simple organic molecules. The chemistry observed in these systems can be conveniently summarized by the following set of basic processes, where R is an alkyl group and X is either a halogen (Cl, Br, I) or a pseudo-halogen (CN, NC, NCO, NCS). The analogous reactions involving dimer radical anions $(RX)_2^{-}$ can also be accommodated by this scheme.

Process			Example
	R• + X⁻ (1a)		CH_3NC (in CD_3CN)
Electron Attachment RX + e⁻ ⇌	[R• --- X⁻] (1b)		CH_3Br (in CD_3CN)
	RX⁻ (1c)		CH_3CN
	R• + X⁻ (2a)		$(CH_3)_3CNCO$
Photodissociation RX⁻ + hν	[R• --- X⁻] (2b)		$(CH_3)_3CNCS$
Thermal Dissociation [R• --- X⁻] $\xrightarrow{\Delta}$ R• + X⁻ (3a)			$(CH_3)_3CI$ (in $(CH_3)_3CNCO$)
Thermal Recovery R• + X⁻ $\xrightarrow{\Delta}$ RX⁻ (4)			CH_3CN

A few generalizations can be made about the scope of these reactions. Electron attachment to alkyl halides is generally found to be dissociative giving rise to either separated fragments as in (1a) or to a radical-anion pair as in (1b). On the other hand, electron attachment to molecules possessing π electron systems is predominantly non-dissociative, as in (1c), although CH_3NC constitutes an exception to this trend. The interconversions of the different paramagnetic species as represented by reactions (2a), (2b), (3a), and (4) are of particular interest. Both the radical anion RX^- and the radical-anion pair $[R\cdot --- X^-]$ can be regarded as intermediate stages in the overall process of dissociative electron attachment. However, if the dissociation of the radical anion is an endothermic process, the fragments produced by photodissociation in (2a) can recombine thermally in (4) to regenerate the radical anion. This type of behavior is exemplified by the nitrile systems.

There is a certain arbitrariness about defining a radical-anion pair in crystalline solids according to the observation of a magnetic resonance interaction between the nominally paramagnetic and diamagnetic fragments. At present it is impossible to state whether the radical-anion pair represents a true minimum in the potential energy curve or merely reflects constraints imposed by the crystalline lattice.

REFERENCES

Adrian, F. J., Cochran, E. L., Bowers, V. A. & Weatherley, B. C., Phys. Rev., 177, 129 (1969).

Atkins, P. W. & Symons, M. C. R., Structure of Inorganic Radicals, p. 257. Elsevier, Amsterdam 1967.

Bonin, M. A., Ph. D. Thesis, The University of Tennessee 1969.

Bonin, M. A., Tsuji, K. & Williams, F., Nature, 218, 946 (1968).

Campion, A. & Williams, F., J. Chem. Phys., 54, 4510 (1971).

Chung, Y. J. & Williams, F., J. Phys. Chem., 76, 0000 (1972).

Chung, Y. J., Takeda, K. & Williams, F., Macromolecules, 3, 264 (1970).

Le Roy, R. J., Sprague, E. D. & Williams, F., J. Phys. Chem., 76, 546 (1972).

Putnam, W. E., McEachern, D. M., Jr. & Kilpatrick, J. E., J. Chem. Phys., 42, 749 (1965).

Takeda, K., Thesis, Kyoto University 1971.

Takeda, K. & Williams, F., Mol. Phys., 17, 677 (1969).

Takeda, K. & Williams, F., J. Phys. Chem., 74, 4007 (1970).

Sprague, E. D., Ph. D. Thesis, The University of Tennessee 1971.

Sprague, E. D. & Williams, F., J. Amer. Chem. Soc., 93, 787 (1971a).

Sprague, E. D. & Williams, F., J. Chem. Phys., 54, 5425 (1971b).

Sprague, E. D., Takeda, K. & Williams, F., Chem. Phys. Lett., 10, 299 (1971).

Wang, J. T., Ph. D. Thesis, The University of Tennessee 1972.

Wang, J. T. & Williams, F., J. Amer. Chem. Soc., 94, 2930 (1972).

LEGENDS TO FIGURES

Figure 1.   ESR spectra and spin density distributions for dimer (left side) and monomer (right side) radical anions of acetonitrile. The upper and lower spectra were obtained using $CD_3C^{14}N$ and $CD_3{}^{13}C^{14}N$, respectively. The dimer and monomer radical anions were produced in Crystal I and Crystal II, respectively, of acetonitrile by γ-irradiation at 77°K in the dark.

Figure 2.   (A)   ESR spectra of γ-irradiated 5 mole % CH_3Br in CD_3CN at 88°K. The upper spectrum was recorded before annealing. The middle and lower spectra were recorded after the sample had been warmed to 175°K for a few seconds. For comparison, the upper and middle spectra were recorded at the same gain whereas the lower spectrum was recorded at half the modulation amplitude and one-tenth the gain.   (B)   ESR spectra of γ-irradiated ca. 10 mole % tert-butyl iodide in tert-butyl isocyanate at 77°K. The upper spectrum was recorded before annealing and the middle spectrum was recorded at the same gain setting after 1 min at 150°K. The lower spectrum was recorded at a reduced gain (X 1/3) after prolonged annealing at ca. 150°K.

Figure 3.   (A)   ESR second-derivative spectra of γ-irradiated tert-butyl isocyanate at 77°K. The upper and lower spectra were recorded at the same gain settings before and after photobleaching with unfiltered

tungsten light. (B) ESR spectra of γ-irradiated crystalline tert-butyl isothiocyanate at 77°K. The upper spectrum was recorded during exposure of the sample to red light (Corning Filter No. 2030) and the middle spectrum during subsequent exposure to unfiltered tungsten light. The lower spectrum was recorded subsequently with the sample in the dark. These last two spectra were recorded at a reduced gain (X 0.8).
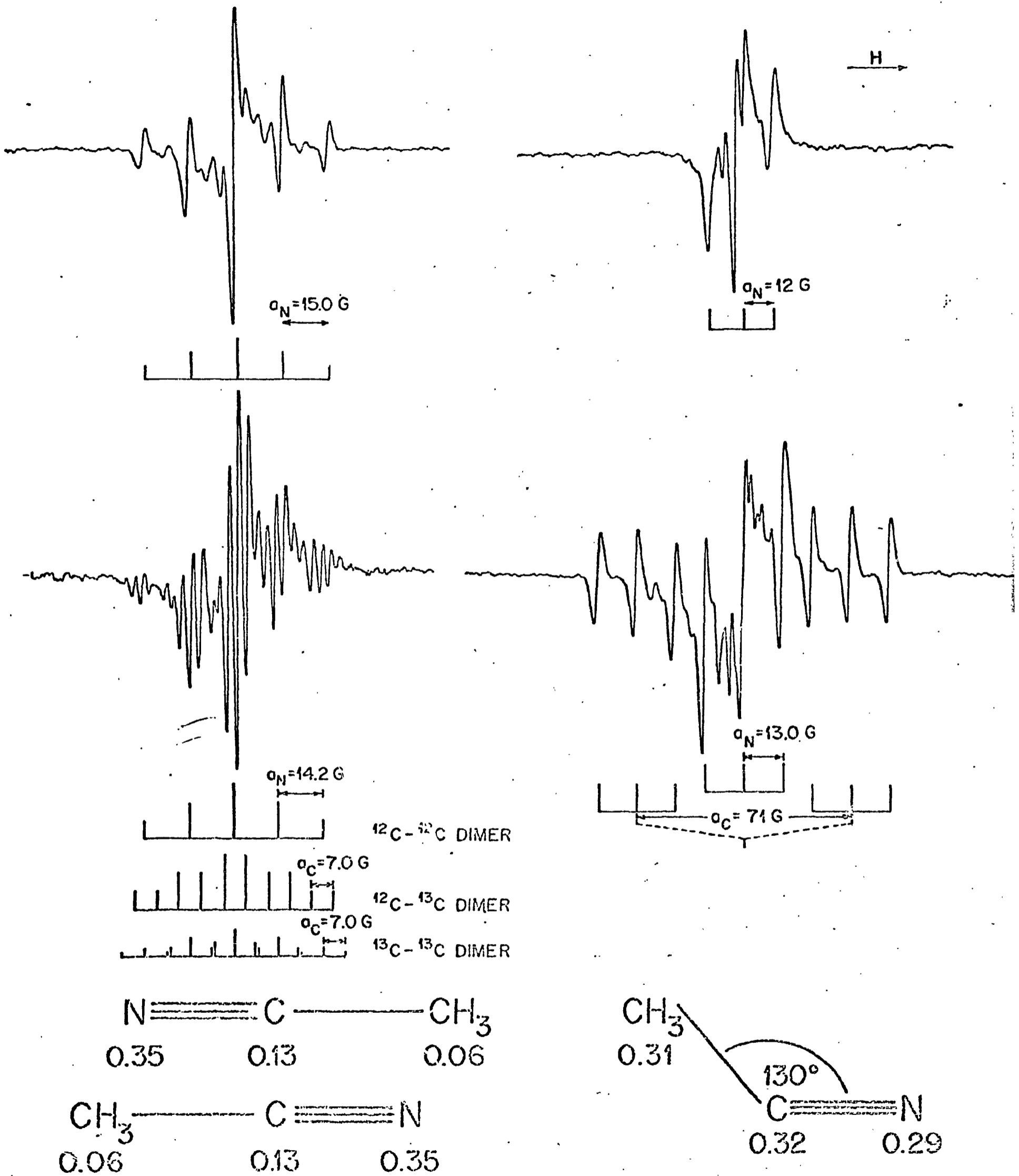
$a_N = 15.0$ G

$a_N = 12$ G

H →

$a_N = 14.2$ G

¹²C – ¹²C DIMER

$a_C = 7.0$ G

¹²C – ¹³C DIMER

$a_C = 7.0$ G

¹³C – ¹³C DIMER

$a_N = 13.0$ G

$a_C = 71$ G

N ≡≡ C ———— CH₃
0.35   0.13   0.06

CH₃ ———— C ≡≡ N
0.06   0.13   0.35

CH₃
0.31

130°
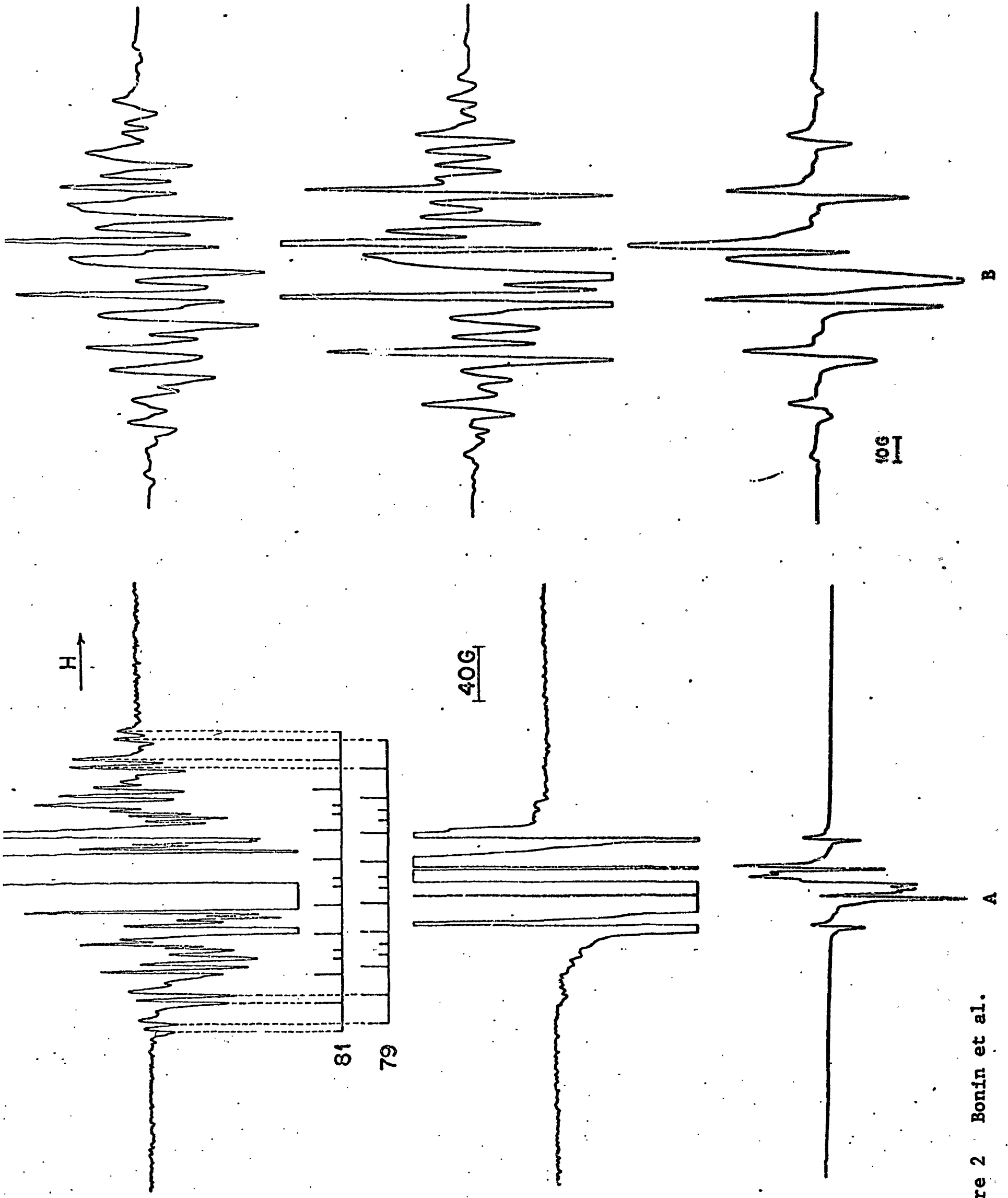
C ≡≡ N
0.32   0.29

Figure 1   Bonin et al.

H→

40G

40G

81
79

B

A

Figure 2   Bonin et al.

Figure 3 Bonin et al.